Journal of Energy Storage 149 (2026) 120078

Contents lists available at ScienceDirect

Journal of Energy Storage

journal homepage: www.elsevier.com/locate/est

Research papers

Essential hydraulic aspects associated with the operation of underground pumped-storage hydropower plants

Berit Finklenburg [a,*], Hillel Rubin [b], Holger Schüttrumpf [a]

[a] Hydraulic Engineering and Water Resources Management Institute, RWTH Aachen University, Aachen, Germany
[b] Faculty of Civil and Environmental Engineering, Technion – Israel Institute of Technology, Haifa, 32000, Israel

ARTICLE INFO

Keywords:
UPSH
Abandoned mines
Hydraulic processes
Operation
Surge wave
Wave damping

ABSTRACT

Pumped-storage hydropower (PSH) is used to store energy by pumping water from a lower source to an upper reservoir. In flat regions, where differences in height are lacking, it is suggested that an underground pumped-storage hydropower (UPSH) plant is built. The objective of this study is to highlight the need to enhance knowledge of hydraulic processes during filling and emptying the lower reservoir of UPSH plants before their construction in abandoned coal-mine areas. This manuscript includes (i) a review of the UPSH concept development, (ii) essential hydraulic aspects associated with the operation of the lower reservoir, and (iii)Model experiments on hydraulic processes during filling and emptying the lower reservoir with a large length-to-height ratio. The model (34.27 m long, 0.212 m high) represents the geometry of coal mine caverns on an approx. scale of 1:35. This is the first physical model to describe the oscillations that occur during the operation of a cavern-shaped lower reservoir. Oscillating single waves with an approximate period of 70 s were observed during the water level rise in the filling process and the drop in the outflow process. Contained oscillations with wave periods of 62–188 s occurred after closing the valve in both processes. The water level of the contained oscillations can be described by a cosine function including an empirically determined wave damping factor, ranging between 1.06 and 1.2. The results show that the discharge determines the performance of the system and may contribute to consideration of the best method to operate tunnel galleries.

1. Introduction

In conventional pumped-storage hydropower (PSH) plants, gravity is used to generate electricity by releasing water from a high reservoir into a lower one [1]. Water is pumped to a higher reservoir during times of low demand and electricity prices. At times of high demand and prices, water is released to drive a turbine in a powerhouse and supply electricity to the grid [2]. Pumped-storage hydropower is the world's largest battery technology, accounting for 96 % of the installed global storage power capacity and well ahead of lithium-ion and other battery types [3]. The rapid growth in variable renewable energy sources, such as solar and wind, has increased the need for stable and reliable storage solutions that can operate at the utility scale [3]. According to the 2025 World Hydropower Outlook of the International Hydropower Association (IHA), the total installed PSH capacity was estimated at 189.4 *GW* in 2024 [4]. Multiple studies have identified the vast potential for pumped-storage sites worldwide [6,7], and there is growing research on the possibilities for different categories of underground pumped-storage hydropower (UPSH) plants, such as retrofitting disused mines, underground caverns, non-powered dams, and conventional hydro plants [8]. Given the resurgence of interest in this technology, with more than 100 PSH projects in the pipeline, the IHA estimates that PHS capacity is expected to increase by nearly 50 % – to approximately 240 *GW* by 2030 [5].

Conventional PSH plants require large vertical differences to be economical and are thus not applicable in flat regions. To overcome this restriction, the application of potential UPSH categories (Fig. 1) should be considered in flat regions [2]. A brief history of UPSH development, which started with the introduction by Fessenden in 1910 [9], was provided by Colas et al. [8] and Yang et al. [10]. In the 20th century, considerations led to excavation of caverns as lower underground reservoirs within hard rocks. Various types of structural lower reservoirs within hard rock geological formations have been considered [11–16]. In the 21st century, the decision to stop mining various types of

* Corresponding author at: RWTH Aachen University, Hydraulic Engineering and Water Resources Management Institute, Mies-van-der-Rohe-Straße 17, 52074, Aachen, Germany.
E-mail address: finklenburg@iww.rwth-aachen.de (B. Finklenburg).

https://doi.org/10.1016/j.est.2025.120078
Received 31 January 2025; Received in revised form 17 December 2025; Accepted 20 December 2025

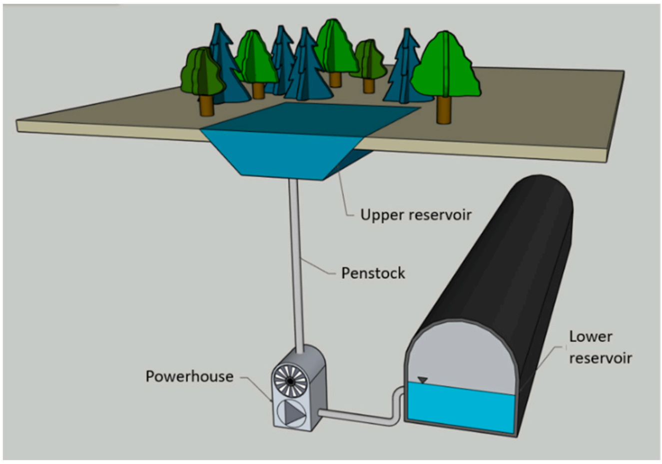

Fig. 1. UPSH plant schematic with a cavern-shaped lower reservoir.

materials led to UPSH categorization, based on the use of abandoned mines as the location of the lower reservoir of the UPSH plant. In particular, the use of coal energy decreased, which led to the abandonment of coal mines in flat regions, such as the Ruhr area in Germany [17,18], the Asturian Central Coal Basin in Northern Spain [19], and the Martelange slate mine in Belgium [20]. Pujades et al. [21] reported (in their study) that in Belgium there were 964 active mines and more than 5000 abandoned mines; and in France there were 4710 active mines and 101,616 abandoned mines. A considerable number of abandoned mines have called for the large-scale utilization of such facilities for UPSH. Yang et al. [10] attest to the great potential of pumped storage combined with abandoned mines (PSAM) due to few geographic constraints and low transformation costs. They have also shown the feasibility of small scale PSAM to solve the problem of instable renewable energy production.

Although the general mode of UPSH operation does not differ from that of conventional PSH, advantages in terms of land use, land consumption, height differences, and public acceptance are expected [8]. UPSH plants in abandoned mines, in particular, obtain economic benefits, reduce disorderly gas discharge, and extent the life-cycle of the mine tunnels and equipment, which might be used in power station construction [10] The disadvantages of UPSH compared to conventional PSH include the shape of the lower reservoir and difficult maintenance [2,8]. The construction of each UPSH plant should be based on a profound set of studies incorporating the chemistry and geology of the formation planned for the lower reservoir and the economic feasibility of the project, including water head and flow capacity ranges [8]. In addition, many issues related to the environment, water quality, and hydraulics must be clarified before an optimal UPSH plant using abandoned mines can be realized [22].

Abandoned coal mines are often cavern-shaped, so their geometry when used as lower UPSH reservoirs greatly differs from this of conventional PSH reservoirs. Hydraulic processes, e.g., water levels and flow velocities, and in particular transient phenomena such as waves and oscillations affect (i) the requirements on the stability of the reservoir walls in terms of pressures and cavitation and (ii) the operation and flexibility services in terms of efficiency and feasibility of rapid operational changes. Thus, hydraulic processes under varying boundary conditions need to be investigated.

This study reviews the development of the UPSH concept (chapter 2), focusses on essential hydraulic topics and processes (especially waves) related to UPSH operation, which should be considered, investigated, and properly addressed to improve UPSH application based on the use of abandoned mines (chapter 3), and firstly experimentally investigates basic hydraulic processes associated with filling and emptying the lower, cavern-shaped reservoir, filling the gap in the literature that was identified in chapters 2 and 3.

2. Development of the UPSH concept

2.1. Lower reservoir excavations for UPSH plants

The intensive energy-saving approach guided by U.S. Presidents during the 1970s and 1980s led the U.S. Department of Energy to support numerous research projects related to UPSH application [12,15,16]. All these studies focused on the UPSH category, where the lower reservoir was excavated within an appropriate hard rock. The conclusions of Tam et al. [12] state: "the technology for UPSH is available, however, additional research and development is required for high-head turbomachinery, motor/generators, caver geology, and system optimization." Additional studies by Tam et al. [12] are ongoing with various additional topics. The results of an extensive research project conducted by Acres American Incorporated [15] indicated that both UPSH and compressed-air energy storage were being seriously considered. The Acres American Incorporated Project [15] referred to excavation in suitable hard rock to prepare the required underground storage. In the same year, Hammet and Hoek [14] discussed the optimal approaches for constructing underground hydroelectric projects with controlled failure mechanisms. Uddin and Asce [23] suggested the use of abandoned deep limestone quarries as underground reservoirs for pumped storage.

Most research projects on UPSH application in the 20th century considered the underground reservoir to be an excavated cavern located in hard rock. Various economic analyses and cost calculations have indicated that minimizing costs for UPSH is primarily associated with reducing the amount of excavation in hard rock and increasing the depth (to the maximum allowable depth by pump–turbo machinery) of the underground reservoir(s). The concept of multiple stages for underground reservoirs is attractive from the standpoint of minimizing site selection requirements and legislative permits. However, UPSH plants incorporate surface reservoirs with proper connections to large shafts, linking two underground reservoirs. Each reservoir comprises a collection of tunnel galleries with drifts that must be properly filled and emptied during UPSH plant operations. All the excavated tunnel galleries drain toward the shafts.

2.2. Using abandoned mines as UPSH lower reservoirs

At the beginning of the 21st century, various research projects considered the possible use of UPSH, using lower reservoirs in disused mines. However, these studies were conducted in Europe. The motivation for these projects originated from the possibility of using the available tunnel gallery volumes of abandoned mines (primarily coal mines) as underground reservoirs. The primary advantage of using coal mines over other mine types is the large number of abandoned coal mines worldwide resulting from energy transition [1,24–26]. Therefore, the potential benefits of reusing these underground spaces for energy storage are significant. In addition, if a UPSH plant in an abandoned coal mine is realized, it could serve as a prototype for other plants with similar site conditions.

Madlener and Specht [17] analyzed the economic aspects of using abandoned coal mines for UPSH plants. Their study referred to the Ruhr area as an example of a possible case in which a UPSH plant could be applied. The upper reservoir can be established at the surface of the former mine without excessive conflict with the settlement areas. The authors claimed that, because of the coal mining technique applied in the Ruhr area, the lower reservoir may have incorporated only some of the existing mine cavities, and new additional caverns should probably be excavated. Madlener and Specht [17] indicated that the cavities or tunnels comprising the lower reservoir should be properly filled and emptied during the UPSH plant operational cycle. They also considered that the surfaces of the tunnels comprising the underground reservoir should be clad with reinforced concrete.

Montero et al. [18] conducted a research project considering exploitation of the abandoned Prosper–Haniel coal mine in the Ruhr region of Germany as the lower reservoir of a UPSH plant. The mine was constructed using seven levels of tunnel galleries interconnected by large shafts. The authors did not provide geotechnical information on the ability of existing tunnel surfaces to resist the various water flow phenomena described later by Pummer [2,27,28] and Pummer and Schuettrumpf [29]. In contrast, Montero et al. [18] considered the possible high head of operation of a pump turbine originating from a maximum depth of 1000 m in the mine. Such a substantial depth implies that the underground storage is divided into two stages. The network of tunnel galleries consists of six levels, each with either a positive or negative slope toward the mine shaft. Tunnels with slopes that do not allow proper drainage toward the shaft cannot be used for UPSH plants. Madlener and Specht [17] applied a one-dimensional flow model for hydraulic analysis of the possible operation of level 6 in the Prosper–Haniel mine. Details of the cycle of filling and emptying the model were not provided; however, it likely referred to steady-state conditions with a Manning's n of 0.015, which refers to the reinforced concrete lining. A tunnel slope < 0.15 % causes difficulties in emptying the tunnel. The experiments showed some difficulties with high head losses in the high discharges during the filling and emptying of the tunnel. The authors suggested that hydraulic issues should be investigated for the improvement and possible implementation of a UPSH plant.

Terrier et al. [30] investigated the behavior of surge waves in the tailrace channels of a common PSH plant with lower and upper above-ground surface reservoirs. Starting and stopping of turbines and pumps can lead to a highly unsteady flow in the tailrace channels of a hydropower plant. Surges and cavitation should be avoided by using pumps and turbines. The same phenomenon should also be considered during the filling and emptying of tunnel galleries in a UPSH plant. Pummer [2,27,28] and Pummer and Schuettrumpf [29] showed by numerical simulations and laboratory experiments the possible development of moving hydraulic jumps and water waves, namely surges and bores, that could be generated during emptying and filling of underground storage tunnels. The development of these waves was reviewed by Chow [31]. Colas et al. [8] outlined three primary factors influencing the decision-making process for the utilization of abandoned mines for UPSH plants: first, stability factors, defined as time-dependent processes resulting from changes in humidity and/or stress re-distribution; second, environmental and human safety, which may be endangered by mine-gas accumulation and water contamination; and third, productivity associated with hydraulic processes, such as water-level oscillations, pressure fluctuations, and variable hydrodynamic pressure, which may affect the discharge within the system.

In recent years, UPSH in combination with abandoned mines gained greater importance in China due to the gradual transformation toward sustainable energy supply. Sun et al. [26] evaluated the regional development potential of UPSH using abandoned coal mines in the Yellow River Basin. They cite the construction investment, reservoir volume, transport conditions and policy support as the most relevant factors for regional development of UPSH plants. Yang et al. [10] investigated the development demand and potential of UPSH in abandoned mines in China. Their research led the authors to attesting the combination of UPSH and abandoned mines considerable social and environmental benefits. The Journal of Central South University published a Special Issue on development and utilization of pumped storage in closed/abandoned mines in 2024, which underlines the increasing importance of UPSH development in China. The articles mainly focus on rock stability issues, however, Yang et al. [32] name waterproofing against impact stresses resulting from the hydraulic processes as one of five key scientific issues in UPSH development in abandoned mines.

3. Essential hydraulic issues

3.1. Pump turbines

The basic operation of a UPSH plant involves the optimal performance of pumps and turbines. Some of the difficulties originating from surges and cavitation in such equipment were outlined by Anderson [33] and Terrier et al. [30] and in greater detail by Giesecke and Mosonyi [34]. Coal-mine depths are often vast, on the order of 1000 m. Typically, pump turbines that operate under such high heads are not available. Therefore, optimal division of the underground storage should be performed, subject to hydraulic and economic calculations. Menendez et al. [35] emphasized the importance of ventilation in the galleries of underground tunnels for the high-efficiency operation of Francis turbines. Pummer [2,27,28] and Pummer and Schuettrumpf [29] stated that proper ventilation of tunnel galleries is also required for diminishing various types of wave reflections and for proper filling and emptying of the tunnel galleries.

3.2. Options for possible use of abandoned mines

Currently, only a few (partial) UPSH plants have been successfully installed [1,36]. However, no abandoned coal mines have been successfully converted into UPSH reservoirs [8].

Madlener and Specht [17] referred to general types of mines in the Ruhr area of Germany. They emphasized that the dominant mining method in the Ruhr area was the long-wall mining technique, which involved the controlled collapse of sediments after coal extraction. The only remnants were drifts that were permanently established for the transportation of input materials, workers, and coal. Existing caverns were particularly created to host technical equipment. Therefore, the authors believe that the remaining cavities from coal mining should be excluded, leaving three options for using an abandoned mine: 1) to excavate and secure additional caverns, 2) to make use of existing drifts, or 3) to dig new drifts. The authors discussed the importance of proper inflow and outflow of all tunnel galleries in an underground reservoir. Montero et al. [18,37] reported that the Ruhr region in Germany incorporated more than 120 mines. Their study focused on the network of tunnel galleries in the Prosper–Haniel mine as a possible lower storage area for a UPSH project. They emphasized the economic advantage of using the available large volume of tunnel galleries and large water head stemming from the deep mining process. They conducted a hydraulic analysis based on the average sizes of the shafts and tunnels existing in the mine. Their hydraulic calculations are as follows:

1) Filling process of underground storage in which shockwaves can be created following the transition of the pump–turbine mode of operation. Shock waves can be generated in adjacent tunnels.
2) Steady-state flow conditions through the tunnels with Manning's n of 0.015, which refers to reinforced concrete, and a slope of 0.2 % to avoid Froude numbers >0.8 to allow a maximum flow velocity of 2.5 m/s.
3) During the emptying process of the underground storage, the turbine discharge gradually decreases to avoid cavitation problems.

Montero et al. [38] provided additional information on the possible use of tunnel galleries in the Prosper–Haniel mine. They found that several tunnel galleries could not be used for pump storage because of their negative slopes to drainage, and very small slopes and volumes. However, sandstone geological formations exist beneath the coal strata. Therefore, coal-mine shafts can be used to excavate caverns in sandstone for expansion of underground pumped storage at lower depths. The operation of the reservoir based on the use of part of the abandoned mine tunnels, together with the additional volume created by sandstone excavation, appeared to be challenging. Combinations of different types of pump–turbines may be required under such circumstances.

Menendez and Loredo [19] suggested using abandoned mines in the Asturian Central Coal Basin in Northern Spain for UPSH plants. Their study suggested a schematic description of a hypothetical UPSH plant operation. Later, in a series of studies, Menendez et al. [35,39–41] addressed various issues associated with underground storage operations. They emphasized several important points, such as the requirement for ventilation, which is crucial for high efficiency of the pump–turbine, as well as for filling and emptying shafts and tunnel galleries. Ventilation also diminished the effects of shockwaves that may have been created during the filling and emptying of the tunnels. The authors identified different modes of oscillation owing to the interference of flows originating from the inflow and outflow of adjacent tunnels.

Pujades et al. [42] discussed the mass exchange between a lower underground reservoir and groundwater. They considered a hypothetical UPSH plant. The lower underground reservoir can be an open-pit mine surrounded by a transmissive porous medium. The transfer exchange between the reservoir and surrounding porous medium was simulated by applying the finite element numerical code SUFT3D to solve Richard's equation. The flow types that were simulated by Pujades et al. [42] to some extent resembled the spatially varied flow in channels [31], namely, overland flow into streams. However, such simulations can differ significantly for different data relevant to actual abandoned mines. Therefore, application of various numerical modeling simulation methods may contribute to improving UPSH knowledge, provided a reference is made to actual data of mines considered for UPSH.

Pujades et al. [21] considered the need for field data to make their modeling approach of 2017 [42] applicable. Thus, Pujades et al. [21] collected field data from an abandoned slate mine located in Martelange, southeastern Belgium, and declared that the abandoned mine could be used for the construction of a UPSH plant. The Martelange mine was developed to extract metamorphic slates from the Lower Devonian Formation of the Ardenne Anticlinorium. The lower reservoir was considered to provide a maximum head of 150 m and was completely submerged below the groundwater surface.

Pummer [2,27,28] and Pummer and Schuettrumpf [29] investigated the processes associated with filling and emptying the tunnel galleries of an underground reservoir, following a hybrid modeling approach with varying operational parameters (flow rate, and depth) and design parameters (branches, changes in direction and cross-section, and slope and roughness). Their experimental and numerical calculations showed that ventilation of the tunnel gallery is crucial. For the structural design (freeboard), knowledge of the maximum water levels is essential, whereas proper operational design (reservoir damping) requires data on the wave velocities and oscillation periods. The authors were the first to distinguish between the global and local flow processes. They defined global processes as time-dependent mean values of measurements, and considered local processes as individual, locally occurring phenomena that arise during operations and superimpose global effects. The filling of the tunnel was accompanied by the creation of moving hydraulic jumps and surges. Employing a tunnel requires minimal drainage slope for efficient underground storage operations.

In China, recent research has aimed to install a tunnel-based UPSH combined with large-scale floating photovoltaic power stations [43].

Huang et al. [44] provided a recent bibliometric analysis of large-scale underground energy storage (LUES). They investigated the development of UPSH research as one of five LUES technologies, with underground gas and hydrogen storage accounting for the highest number of publications over the previous few years, whereas UPSH has played a minor role in recent LUES publications. This contrasts with the significance of conventional PSH, which is a primary global energy storage technology. This gap underlines the potential for future UPSH usage and the need for further research to move UPSH from a prospective to a mature technology. Furthermore, analysis of UPSH-related keywords showed that hydraulic processes and experimental models have not been significantly considered in recent publications.

This gap in the literature highlights the necessity for more focused research on the hydraulic processes associated with UPSH. To address this, physical model experiments were conducted in this study to better understand these processes. These experiments are essential for advancing the design and operation of UPSH systems, providing valuable insights into the behavior of hydraulic flows and their impact on the overall system efficiency.

3.3. Waves in cavern-shaped reservoirs

Operation of UPSH plants in abandoned coal mines is associated with frequent flow changes in the lower, tunnel-shaped reservoir, initiated by starting and stopping the filling and emptying process. Due to the ventilation of the reservoir, the flow corresponds to an open channel flow, until it reaches the end of the channel. Surface waves in open channels are non-stationary movements. We distinguish between oscillatory and translational waves. Oscillatory waves describe surface waves, which are not associated with mass transport in horizontal movement direction, but only with energy transport. Only at low flow depth, e.g., when an ocean wave approaches the coast, translational movement occurs. Translational waves, on the other hand, result from discontinuous flow changes, e.g., due to valve opening or closing. These waves are described as surge and sunk waves, depending on the water level rise or drop [45]. Surge waves in UPSH tunnel reservoirs occur during the filling process and at the end of the emptying process, while sunk waves result from opening the valve at the beginning of the emptying process and from closing the valve at the end of the filling process. The physics of surge and sunk waves in open channels are described in detail by Aigner and Bollrich [46]. Neglecting the oscillating surge and sunk waves, the water level in the reservoir during the filling and emptying process might be described by linear functions, if the flow rate is constant.

In between the two operational processes of a UPSH reservoir (filling and emptying), the reservoir may be closed and is hence considered a closed basin. Resulting from the closing of the valve, the surge and sunk waves move through the flume while being damped. The water level in the reservoir under these conditions might be described by Eq. (1), which originates from the classical structural motion equation for a single degree of freedom [47]:

$$h(x,t) = h_T + H cos\left(\frac{2\pi}{T}t\right) cos\left(\frac{2\pi}{L}x\right) e^{-\xi\omega_D t} \tag{1}$$

where

$$\begin{aligned} &h_T = target\ final\ water\ level\ [m] \\ &H = wave\ height\ of\ the\ first\ wave\ [m] \\ &T = wave\ period\ [s] \\ &L = length\ of\ the\ flume\ [m] \\ &\xi = \frac{1}{2\pi} \bullet ln(\delta) \\ &\delta = wave\ damping\ factor\ [-] \end{aligned} \tag{2}$$

$$\omega_D = \omega\sqrt{1-\xi^2} \tag{3}$$

$$\omega = \frac{2\pi}{T} \tag{4}$$

The condition of the wave at the time of operational change may affect the following operational process. Thus, in a first step, we need to know, how the waves behave during the single processes, and during operational changes (i.e., a closed basin condition).

4. Experiments and instrumentation

The aim of the experiments is to understand basic hydraulic processes in lower, cavern-shaped reservoirs of UPSH plants during the filling and emptying processes. Compared to economic and geological considerations, hydraulic processes have not yet been focused on intensively in recent research. However, knowledge on wave properties and water levels within the reservoir is crucial for (i) dimensioning the reservoir walls with regard to pressure resistance, and (ii) a save operation of a UPSH plant. Thus, an experimental model was set up to investigate relevant processes and develop equations describing waves and water levels.

The experiments were conducted in a 34.27 m long and 141 mm wide flume made of acrylic glass, representing the lower reservoir of a cavern-shaped UPSH plant (Fig. 2). The geometry was designed to represent the typical shape of an abandoned mine yet did not represent a specific mine. In addition, prior investigations have shown that a single flume with a large length-to-height ratio has a negative impact on the system behavior in terms of the freeboard, effective usable storage capacity, wave damping properties, and overall behavior during operational changes [48]. Thus, the model represents the most unfavorable design for a UPSH lower reservoir to obtain potential improvements and gain information on an optimal design [49]. The flume cross section was composed of a square and a semicircle with a radius of 71 mm. The inflow into the model passed through a polyvinylchloride pipe with an inner diameter of 57 mm inclined at an angle of 30°. The pipe can be connected to a cylindrical surge tank with an inner diameter of 0.19 m and a height of 0.96 m. However, prior investigations did not show an optimization of hydrodynamical processes due to the implementation of the surge tank [49]. Thus, it was not used in the present study. The pipe was equipped with two rotary valves, the degrees of which were controlled to obtain different flow rates. A diffuser connected the pipe to the flume and provided a transfer from pressure to free-flow. Water was pumped from the reservoir into the flume using a block pump (KSB Etachrom B, KSB SE & Co. KGaA, Frankenthal, Germany, with a maximum flow rate of 16.67 L/s and a maximum pressure head of 32 m). Water was drained from the model using gravity. The amount of water running into and out of the model was measured by an ultrasonic flow meter (UFM) (AquaTrans™ AT600, Baker Hughes Company, Houston, TX, USA) with ±1 % measuring accuracy. Ultrasonic sensors (USSs) (microsonic mic+35/IU/TC, microsonic GmbH, Dortmund, Germany) with ±1 % measuring accuracy for measuring the water level in the flume were installed at four positions, with two sensors at the inflow cross section, one in the middle section and one at the end section. Measuring frequency was 5 Hz. Using the timestamp of the first water-level increase and the distance between the USSs, the inflow velocity of the first wave was calculated.

A total of 25 experiments was conducted to investigate the basic hydraulic processes occurring during the filling and emptying of the lower reservoir. In the experiments, the inflow and outflow rates were varied from 1 to 5 L/s. The initial and final water levels varied from 0/11 to 4/13 cm (Table 1). The initial and final water levels of the filling process were the same, and vice versa for the emptying process. For

Table 1
Experimental plan. Five tests each with identical initial/final water level and changing flow rate of 1, 2, 3, 4 and 5 L/s.

Test no.	Initial water level inflow/ final water level outflow [cm]	Final water level inflow/ initial water level outflow [cm]	Flow [L/s]
1	0	11	1
2	0	11	2
3	0	11	3
4	0	11	4
5	0	11	5
6*	0	11	1
7*	0	11	2
8*	0	11	3
9*	0	11	4
10*	0	11	5
11*	0	11	1
12*	0	11	2
13*	0	11	3
14*	0	11	4
15*	0	11	5
16	2	13	1
17	2	13	2
18	2	13	3
19	2	13	4
20	2	13	5
21	4	15	1
22	4	15	2
23	4	15	3
24	4	15	4
25	4	15	5

*Repetitions of tests 1–5 for evaluating reproducibility

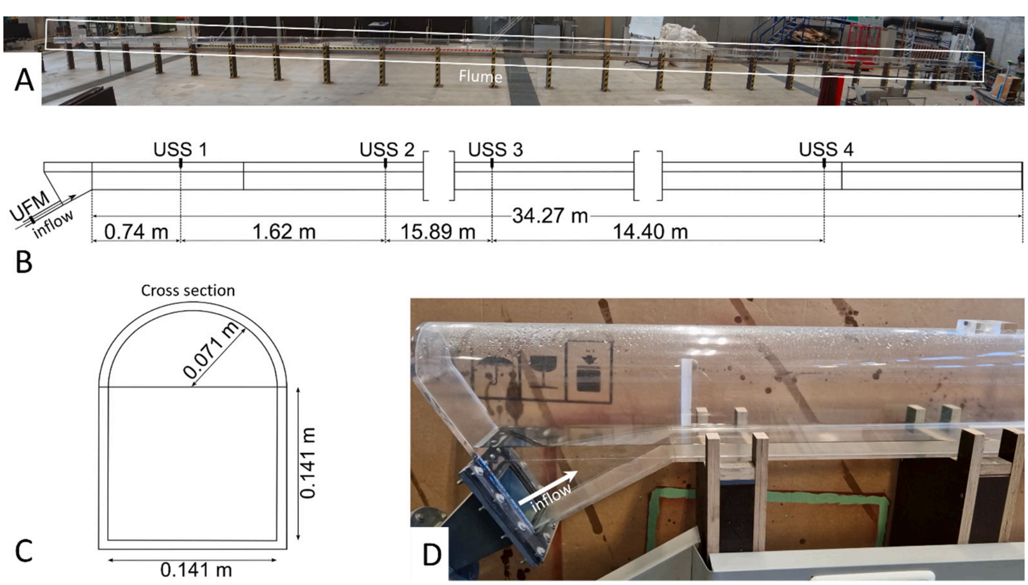

Fig. 2. Model of the UPSH lower reservoir in the hydraulic lab at RWTH Aachen University. A: full model (photo); B: full model (scheme, side view with measuring instruments); C: cross section (scheme); D: inflow area side view (photo).

evaluating the reproducibility of the experiments, three test series were conducted with an initial water level of 0 cm (test nos. 1–15).

In the inflow tests, the pump was started with a lead time of approximately 10 *s* before the valve was opened. The targeted flow was achieved after approximately 50 *s*. In outflow tests, the target flow was achieved after approximately 20 *s*.

The data generated by the model tests were processed and analyzed using Matlab©, Version R2022b (the MathWorks, Inc., Natick, MA, USA). The runtime was adjusted such that every experiment began immediately at the time of valve opening, that is, the valve was opened by >5 %. Outliers were linearly replaced based on the moving mean with an interval of 100. The time at which the inflow wave passed through the USSs was detected using a threshold value that varied according to the initial conditions of each experiment. The velocity of the inflow wave between the two sensors was then calculated by dividing the distance between the sensors by the time the wave needed to move from one sensor position to the next. To calculate the wave periods during the wave-damping periods, the data were smoothed with a span of 50 data points to identify the local peaks, and the time between two successive peaks was calculated and averaged, resulting in the mean-wave period.

Although the model was not based on a specific abandoned mine, it was transferred to the order of magnitude of cavern-shaped mines on a scale of 1:35 using Froude's model law, which states that the ratio of inertial forces to gravitational forces must be identical for model and nature scale. Thus, the dimensionless Froude number must be the same in model and nature:

$$Fr_{Model} = Fr_{Nature} = \frac{v}{\sqrt{g \bullet h}} \tag{5}$$

where

$v = flow\ velocity \left[\frac{m}{s}\right]$

$g = gravity \left[\frac{m}{s^2}\right]$

$h = flow\ depth\ [m]$

The dimensions and parameters of the model and natural scales are listed in Table 2.

The experimental results are provided on a model scale and may be transferred to the scale of a specific mine that could be used for a UPSH plant, considering scale and model effects.

Table 2
Channel dimensions and primary parameters in model and natural scales, transferred according to Froude's model law.

Parameter	Symbol	Value (model)	Unit	Value (natural)	Unit
Channel width	w	0.141	*m*	4.935	*m*
Channel height	h	0.212	*m*	7.42	*m*
Channel length	l	34.27	*m*	1199.45	*m*
Min. flow	Q_{min}	1	*L/s*	7.25	m^3/s
Max. flow	Q_{max}	5	*L/s*	36.24	m^3/s
Min. flow velocity	v_{min}	0.4	*m/s*	2.37	*m/s*
Max. flow velocity	v_{max}	1.2	*m/s*	7.1	*m/s*
Min. flow depth	$h_{w,min}$	0.02	*m*	0.7	*m*
Max. flow depth	$h_{w,max}$	0.15	*m*	5.25	*m*
Min. Reynolds number	Re_{min}	45,802	–	9,483,792	–
Max. Reynolds number	Re_{max}	1,374,046	–	284,513,761	–
Min. Froude number	Fr_{min}	0.34	–	0.34	–
Max. Froude number	Fr_{max}	1.84	–	1.84	–

Each model is influenced by the scale and model effects. Scale effects result from the impossibility of fulfilling all the relevant similarity laws in a scaled experiment, whereas model effects result from the inability to fully reproduce reality in the model. Both effects must be considered regarding the transferability of the experimental results from the model to the prototype. However, the scale effects can be assumed to be minimal owing to the certainty of turbulent flow, sufficiently high water depths, and similar flow conditions in all flow sections of the channel [50]. Real-life scenarios may differ significantly from the selected UPSH layouts, resulting in model effects. Hence, additional numerical or experimental investigations are required, depending on the final design, geometric and hydraulic properties, and energy storage constraints of the UPSH plant. Therefore, the following experimental investigations can be used as starting points for the preliminary design of UPSH plants.

A numerical model with an identical geometry to the experimental model is currently being developed at RWTH Aachen University and may serve to investigate the effect of the geometric parameters on the hydraulic processes in the flume.

5. Results

In this study, the inflow and outflow of the lower reservoir were examined separately as individual processes without mutual interference. This indicates that the initial and final water surfaces in each experiment were smooth. In the example of initial and final water levels of 0 and 11 *cm*, respectively, we conducted three experiments with identical boundary conditions. The results showed good agreement; therefore, we rated the reproducibility as sufficient to avoid repetition in further tests.

5.1. Inflow processes

Regardless of the flow volume into the model and the initial water level, the inflow process was subdivided into two stages: first, the filling itself, while the valve was open, and the water level and volume in the reservoir increased (Phase 1); second, the phase of gradually decaying oscillations that developed along the flume after closing the valve (Phase 2).

At the beginning of the first phase, when the pump was started and the valve was opened, the initially smooth water surface bulged upward until the water surface showed turbulence (Fig. 3). Subsequently, the water flowed into the flume, forming a surge wave, followed by single waves.

While proceeding through the flume, the height and velocity of the surge wave decreased owing to wall friction. The wave remained as a surge wave until it was reflected at the end of the flume and dissipated into single waves during backflow (Fig. 4).

At low flow rates (1 and 2 *L/s)*, the first phase can be further subdivided into the first surge wave (Phase 1A, Fig. 5) and the phase with a relatively constant water level increase (Phase 1B). The latter phase began when the first surge wave dissipated into single waves and returned to the inflow section of the flume. At higher flow rates (3–5 *L/s*), Phase 1B did not occur or occurred for a very short time (< 60 *s*) because the targeted flow depth was (or was almost) reached when the surge wave returned to the inflow section.

5.1.1. Phase 1A – surge wave

The inflow surge wave proceeded through the flume at a decreasing flow velocity. At an initial water depth of $h_0 = 0\ cm$, the surge wave reached the end section of the flume after approximately $T = 70\ s$ (for Q = 5 *L/s*) to $T = 110\ s$ (for Q = 1 *L/s*, Fig. 6). The flow velocity of the surge wave ranged from 0.54 *m/s* (Q = 1 *L/s*) to 1 *m/s* (Q = 4 *L/s*) at the inflow section and 0.4 *m/s* (Q = 1 *L/s*) to 0.7 *m/s* (Q = 4 *L/s*) at the end section of the flume (Fig. 6, right).

For an initial water depth of $h_0 = 2\ cm$, the surge wave reached the end section of the flume after approximately $T = 50\ s$ (Q = 5 *L/s*) to $T =$

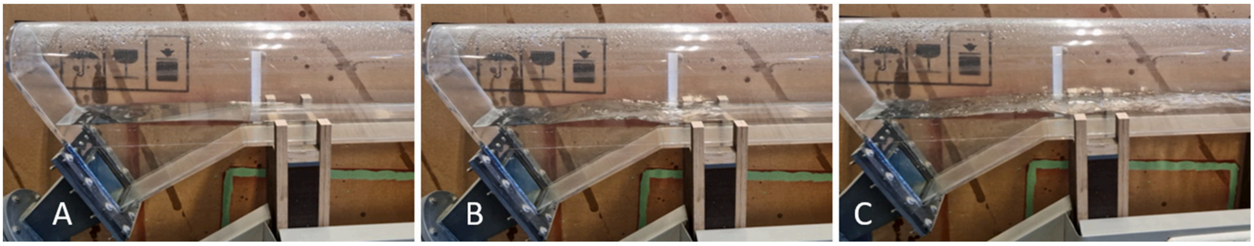

Fig. 3. Start of the inflow test at the inflow area of the model. A: smooth surface bulged upward; B: turbulence occurred at the water surface; C: water flowed into the channel.

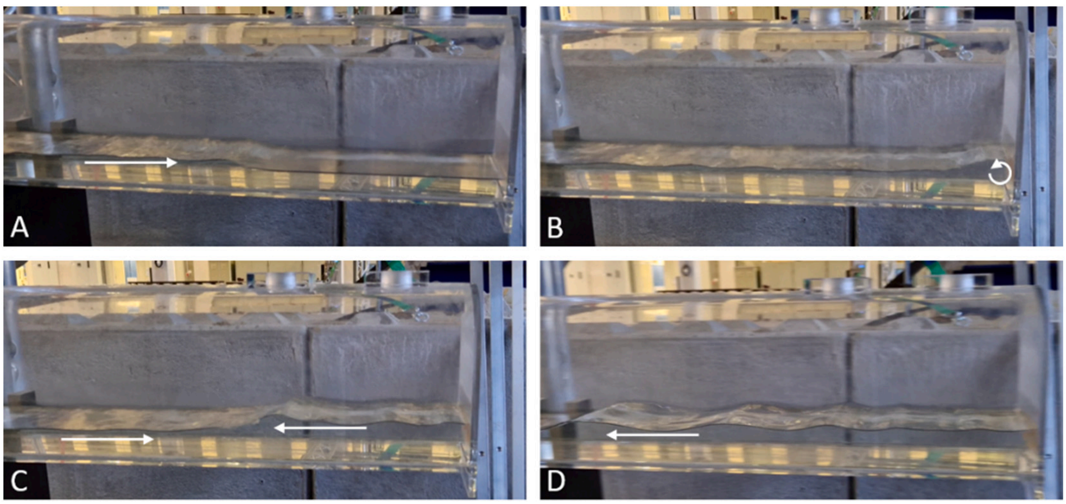

Fig. 4. Reflection of the surge wave at the end of the flume. A: surge wave approaches end of flume; B: reflection; C, and D: backflow of dissipated single waves.

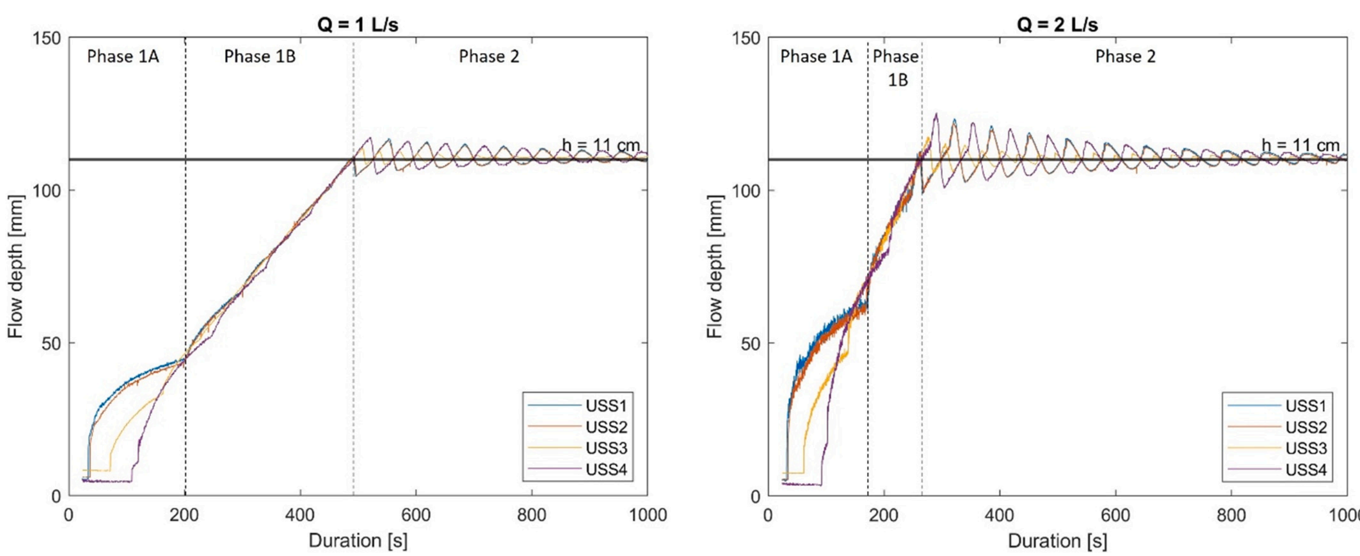

Fig. 5. Flow depth over time during the inflow recorded by four ultrasonic sensors (USS1–4). Phase 1A: Inflow surge wave traveling through the flume, until it returned to the inflow section; Phase 1B: relatively constant water level increase, while the valve was open; Phase 2: gradually decaying oscillations after closing the valve. Left: Q = 1 L/s, h_0 = 0 cm; right: Q = 2 L/s, h_0 = 0 cm.

70 *s* (Q = 1 *L/s*). The inflow velocity in this example varied between 0.9 *m/s* (Q = 1 *L/s*) to 0.98 *m/s* (Q = 5 *L/s*) at the inflow section of the flume and 0.6 *m/s* (Q = 1 *L/s*) to 0.83 *m/s* (Q = 5 *L/s*) at the end section of the flume (Fig. 7).

At an initial flow depth of $h_0 = 4$ *cm*, the surge wave passed through the flume in T = 50 *s* (Q = 5 *L/s*) to *T* = 63 *s* (Q = 1 *L/s*), which corresponded to flow velocities of approximately 1.07 *m/s* (Q = 1 *L/s*) to 1.18 *m/s* (Q = 5 *L/s*) at the inflow section and 0.73 *m/s* (Q = 1 *L/s*) to 0.92 *m/s* (Q = 5 *L/s*) at the end section of the flume (Fig. 8).

5.1.2. Phase 1B – constant water level increase

After the first surge wave returned to the inflow section, the water

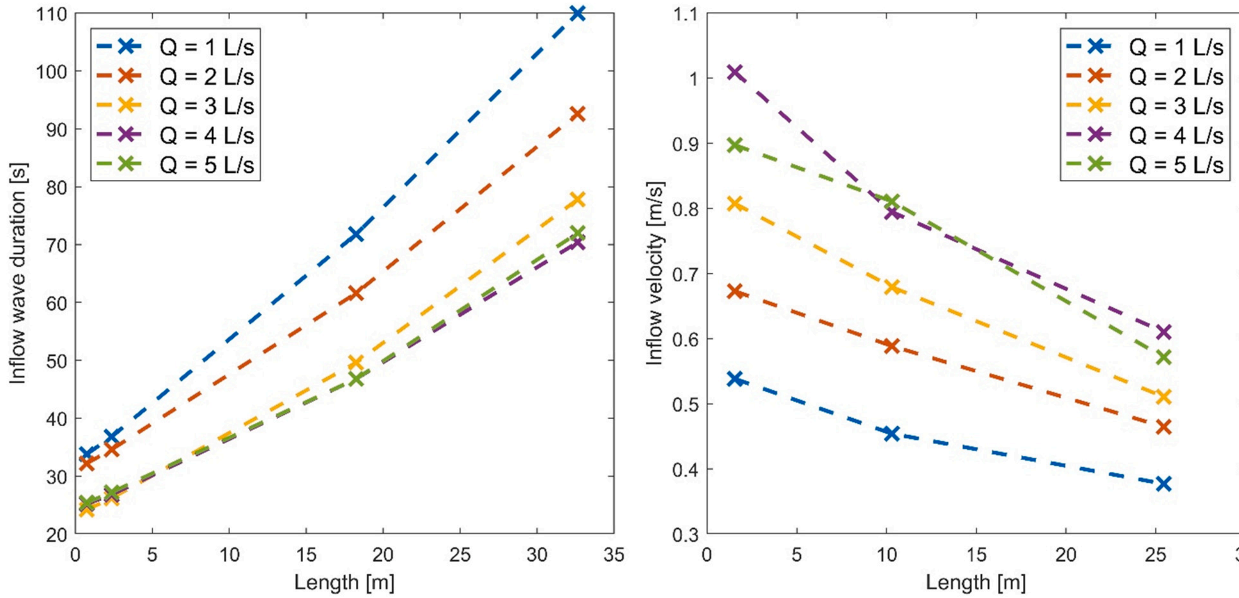

Fig. 6. Inflow wave duration (left) and, inflow velocity (right) over the channel length for experiments with $h_0 = 0$ cm.

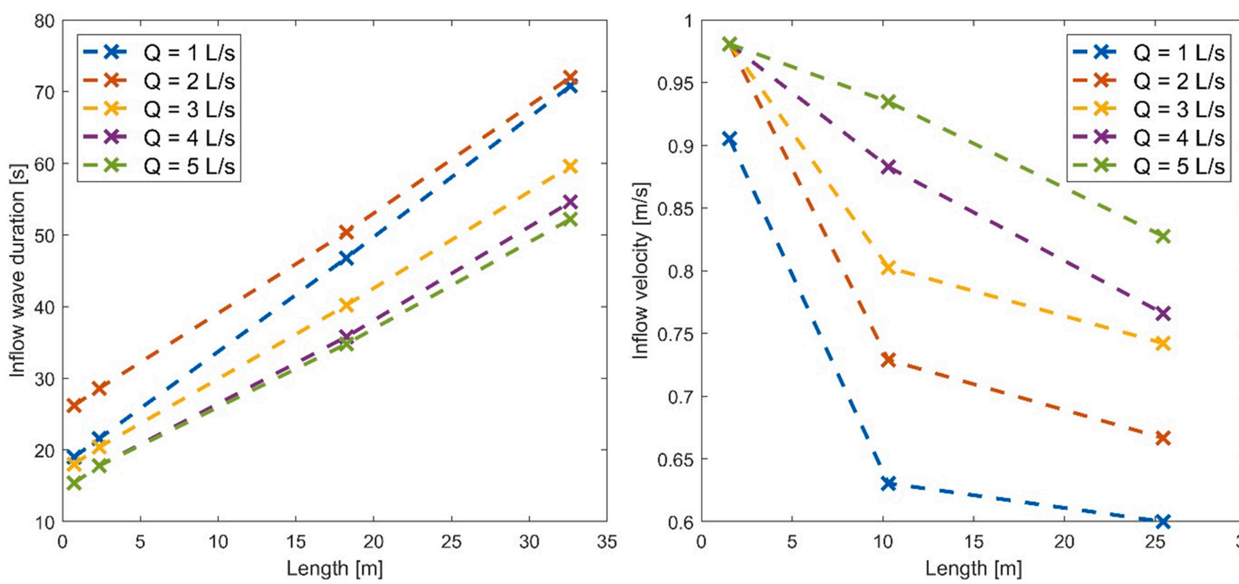

Fig. 7. Inflow wave duration (left) and, inflow velocity (right) over the channel length for experiments with $h_0 = 2$ cm.

level in the flume increased at a constant rate, with the gradient of the flow depth corresponding to the flow rate. However, subtracting the average slope of the water level from the actual flow depth for each measured value revealed oscillations that gradually decayed over time (with increasing water level). At the initial water depth of $h_0 = 0$ *cm* and Q = 1 *L/s* (Fig. 9, left), oscillations of up to 3.3 *mm* in the inflow section (USS1, and USS2) and up to 3 *mm* at the end section of the flume (USS4) occurred. They decayed to approximately 1.5 *mm* (at USS1 and USS2), and 1 *mm* (at USS4). In the middle section of the flume (USS3), the oscillations did not exceed 1 *mm*. The duration of Phase 1B in this example was approximately 300 *s*. With Q = 2 *L/s*, the constant filling phase took approximately 90 *s* and the oscillations ranged from <3 *mm* in the middle section of the flume to over 7 *mm* at its end section and 8 *mm* at the inflow section (Fig. 9, right).

Increasing the initial water level to $h_0 = 2$ *cm* (Fig. 10) resulted in an extended phase 1B duration, combined with higher oscillations. In the experiment with Q = 1 *L/s*, the duration was 350 *s* with oscillations ranging from 1.5 *mm* in the middle section of the flume, to 4 *mm* at the inflow and end sections of the flume. At Q = 2 *L/s*, the duration was 130 *s*, and the oscillations varied between 3 *mm* in the middle section and 8 *mm* in the inflow section.

In the experiments with an initial water level of $h_0 = 4$ *cm*, the Phase 1B duration remained approximately the same as that of $h_0 = 2$ *cm*, whereas the oscillation ranges increased. For $Q = 1$ *L/s*, the oscillations ranged from 4 *mm* in the middle section of the flume to approximately 10 *mm* in the inflow and end sections. For $Q = 2$ *L/s*, the oscillations reached 11 *mm* at the inflow section, 4 *mm* in the middle, and 10 *mm* in the end sections, respectively (Fig. 11).

5.1.3. Phase 2

Phase 2 of the inflow process began when the valve was closed; thus, the inflow stopped. The pump was switched off after closing the valve. As a result of the valve closure, a sunk wave developed and oscillated through the flume. Although the wave height decreased over time owing

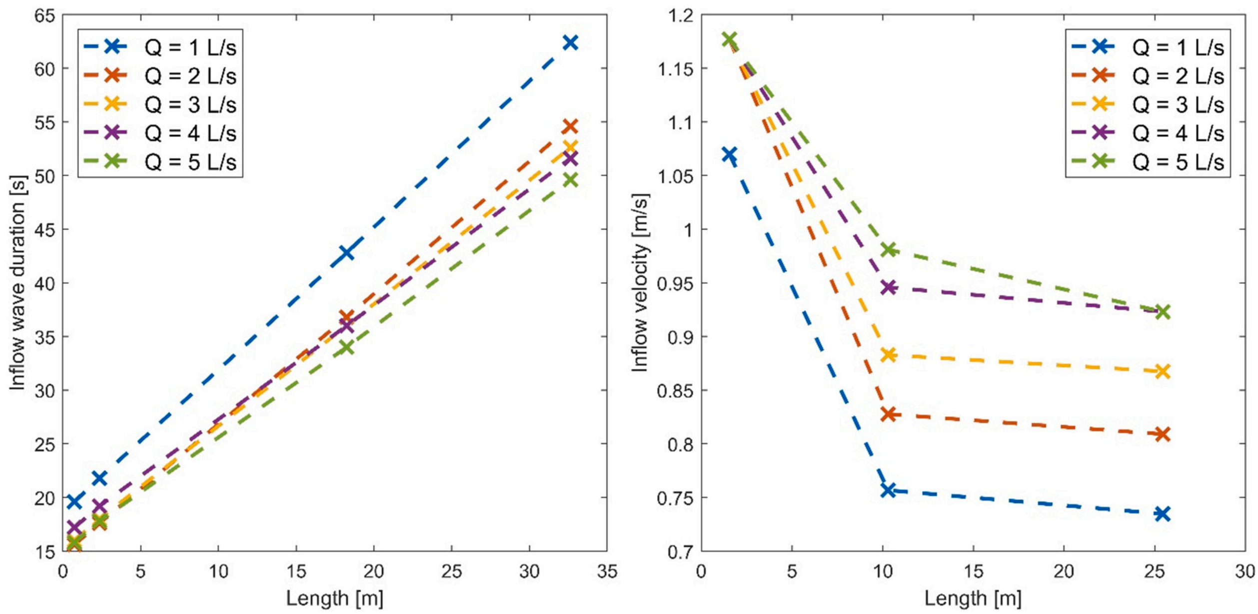

Fig. 8. Inflow wave duration (left) and, inflow velocity (right) over the channel length for experiments with $h_0 = 4$ cm.

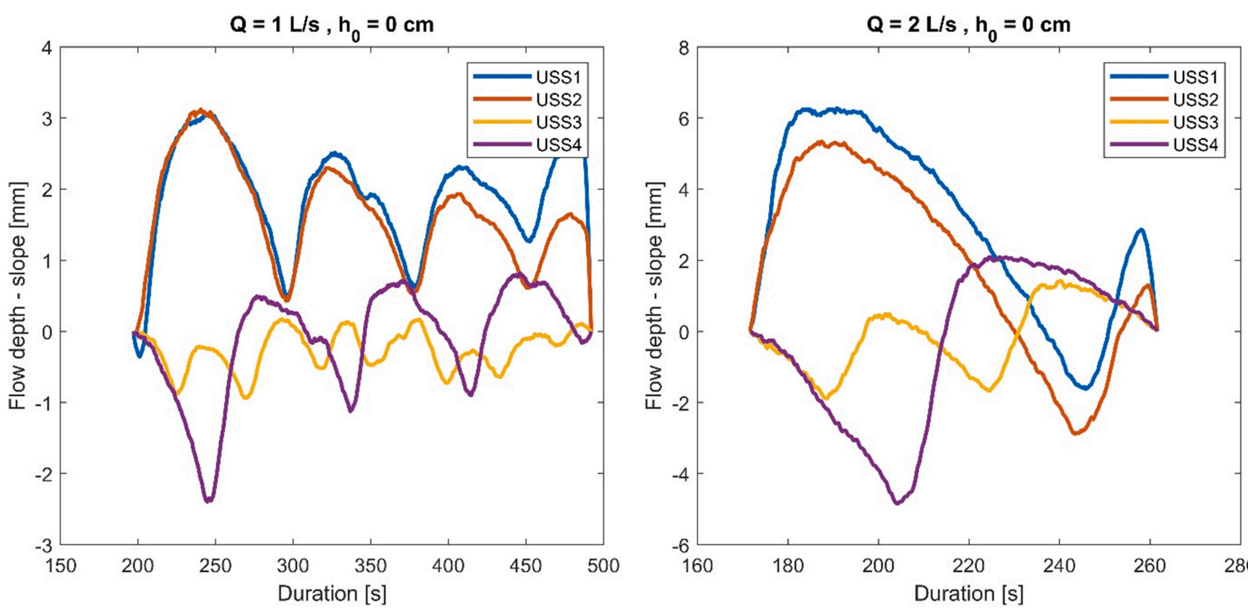

Fig. 9. Oscillations during inflow phase 1B for $h_0 = 0$ cm. Left: Q = 1 L/s; right: Q = 2 L/s.

to friction with the flume walls, the wave period remained constant and did not vary significantly with the varying flow rates (maximum deviation from the mean of all flow rates of 3.51 % at 5 L/s and $h_0 = 0$ cm, s. Fig. 12. When neglecting 5 L/s, the maximum deviation is 0.62 %). At $h_T = 11$ *cm*, the wave period in the middle section of the flume (USS3) was approximately 34 *s*. At the inflow and end sections of the flume, the sunk wave was superposed owing to the reflection from the flume walls, with wave periods of approximately 68 *s*, which was twice the value of the period in the middle section of the flume (Fig. 12). For $h_T = 13$ *cm*, the wave periods reached values of approximately 31 *s* in the middle section of the flume and 62 *s* in the end and inflow sections.

5.2. Outflow processes

The outflow process was subdivided into two phases: first, a relatively constant mean water-level decrease, and second, depending on the target final water level, a logarithmically decaying water-level decrease approaching zero (Fig. 13) or a surge wave oscillating through the flume and gradually decaying to a smooth final water level not equal to zero. The first phase ended when the water column in the inflow section decreased and the inlet pipe was subjected to aeration, or when the valve was closed and a surge wave developed.

5.2.1. Phase 1 – constant outflow

When the outflow valve was opened, sunk waves developed and oscillated through the flume. Although the sunk wave was significant in the data, it was not clearly recognizable to the naked eye during the experiments. In addition to the oscillations, the mean water-level decrease during Phase 1 was relatively constant. For $h_0 = 11$ *cm* and $Q = 1$ *L/s*, Phase 1 ended approximately 300 *s* after opening the valve. For $Q = 2$ *L/s* and $Q = 3$ *L/s*, Phase 1 took approximately 150 *s* (Fig. 13). At higher flow rates, Phase 1 ended before the sunk wave reached the

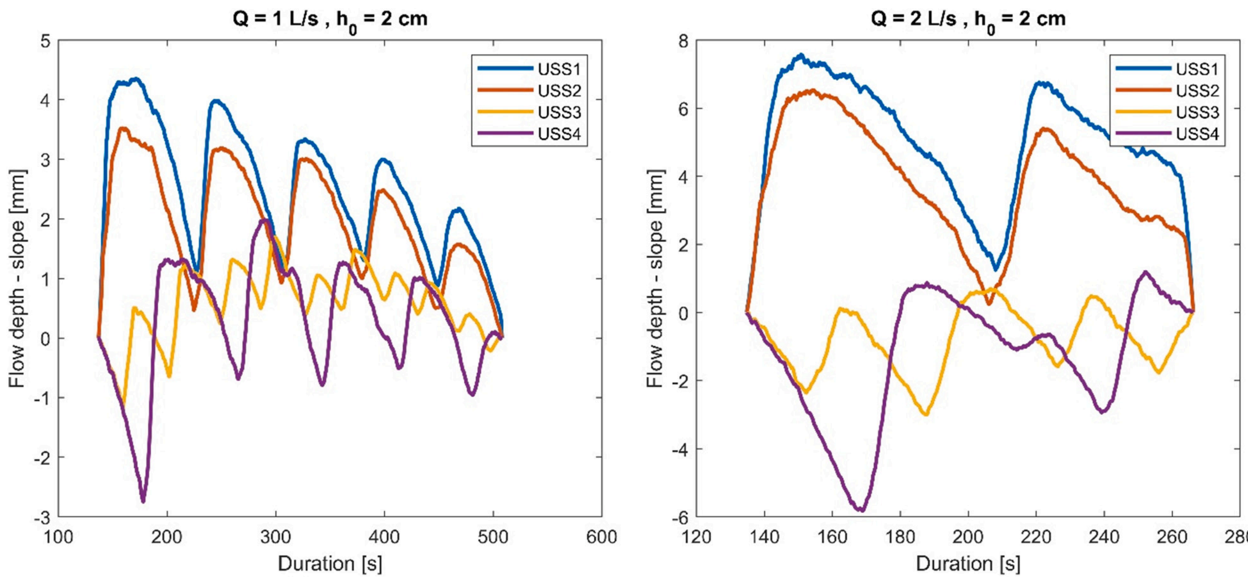

Fig. 10. Oscillations during inflow Phase 1B for h_0 = 2 cm. Left: Q = 1 L/s; right: Q = 2 L/s.

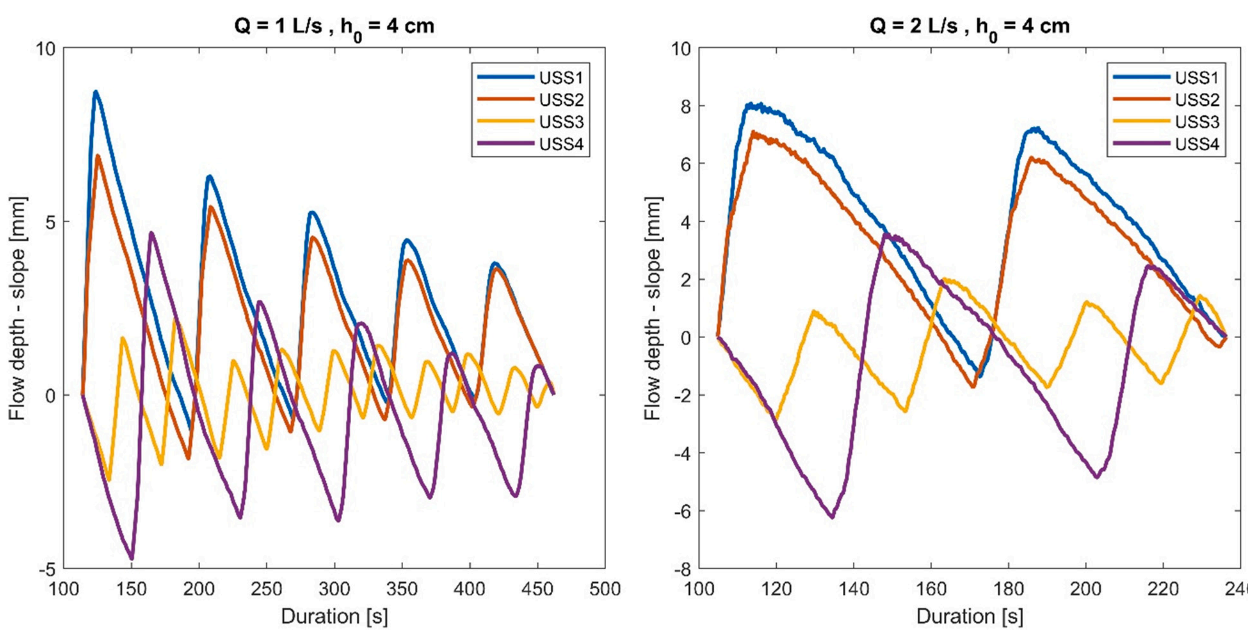

Fig. 11. Oscillations during inflow Phase 1B for h_0 = 4 cm. Left: Q = 1 L/s; right: Q = 2 L/s.

end section of the flume. Therefore, the phases were overlaid and could not be clearly separated.

Sunk waves proceeded through the flume at varying flow velocities. The time of the wave and the corresponding velocity were calculated for the first water-level decrease detected by the USSs. For the initial water level of $h_0 = 11$ *cm* and flow rates of 1–4 *L/s*, the sunk wave reached the end section of the flume after approximately 45–50 *s*, and for $Q = 5$ *L/s* after 40 *s* (Fig. 14). The flow velocity of the sunk wave ranged from 1.3 *m/s* (Q = 1 *L/s*) to 1.7 *m/s* (Q = 5 *L/s*) in the inflow section and remained relatively constant at 1 *m/s* from the middle to end sections of the flume, regardless of the flow rate.

Increasing the initial water level led to a slight increase in the flow velocity. At $h_0 = 13$ *cm*, the sunk wave reached the end section of the flume after approximately 40 *s*, regardless of the flow rate (Fig. 15). The corresponding velocity ranged from 1.47 *m/s* (Q = 3 *L/s*) to 1.69 *m/s* in the inflow section to approximately 1.1 *m/s* (all tested flow rates) at the end section of the flume with a slightly lower flow velocity in the middle section of the flume.

In the experiments with an initial water level of $h_0 = 15$ *cm*, the sunk wave behaved similarly to that of $h_0 = 13$ *cm* (Fig. 15).

Similar to the filling process, the oscillations during emptying can be extracted by subtracting the mean water level from the water level at the individual ultrasonic probes. At the initial water depth $h_0 = 11$ *cm* and Q = 1 *L/s* (Fig. 16, left), oscillations of approximately 10 *mm* occurred at the inflow sections (USS1, and USS2) and at the end section of the flume (USS4). The oscillations gradually decreased to approximately 5 *mm* after 300 *s*. In the middle section of the flume (USS3), the oscillations decreased from 4 *mm* at the start of Phase 1 to <1 *mm* at the end of this phase. For $Q = 2$ *L/s* (Fig. 16, right), oscillations of up to 20 *mm* occurred at the inflow and end sections of the flume, whereas they ranged up to 8 *mm* in the middle section. As only one full oscillation of the sunk wave appeared before the end of Phase 1, the decay of the oscillations could

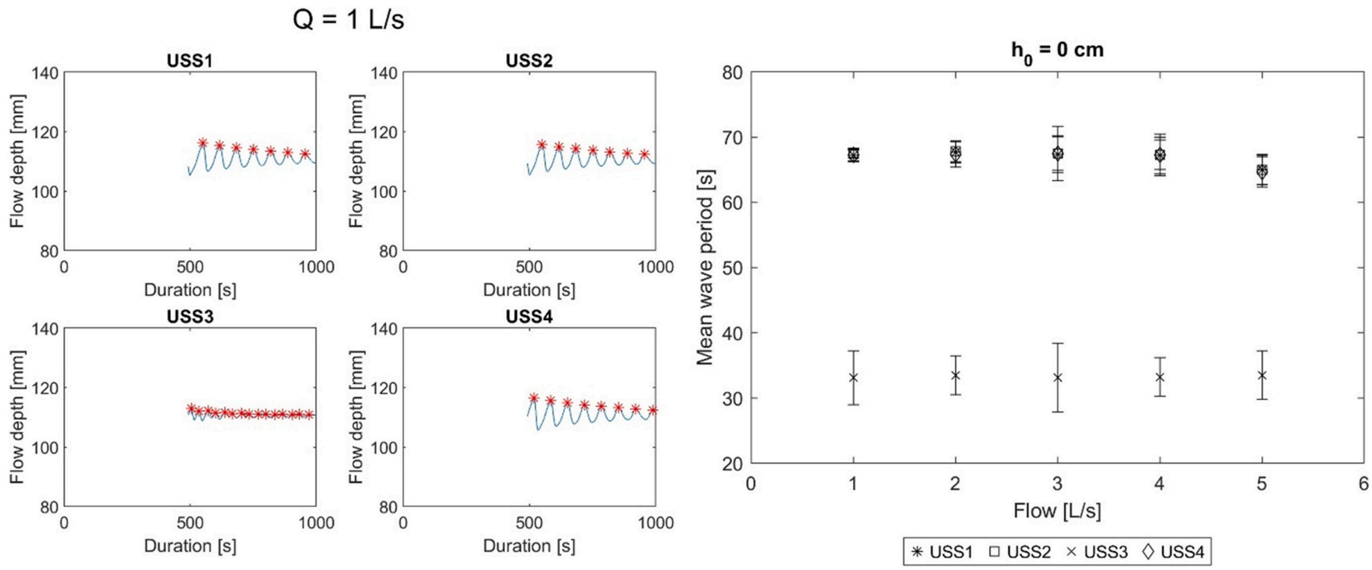

Fig. 12. Phase 2 of the filling of the underground pumped storage reservoir model. Left: The flow depth over time in Phase 2, data is smoothed, and peaks are highlighted with red asterisks; right: mean-wave periods and standard deviations at each ultrasonic sensor position for all flow rates and $h_0 = 0$ cm. (For interpretation of the references to colour in this figure legend, the reader is referred to the web version of this article.)

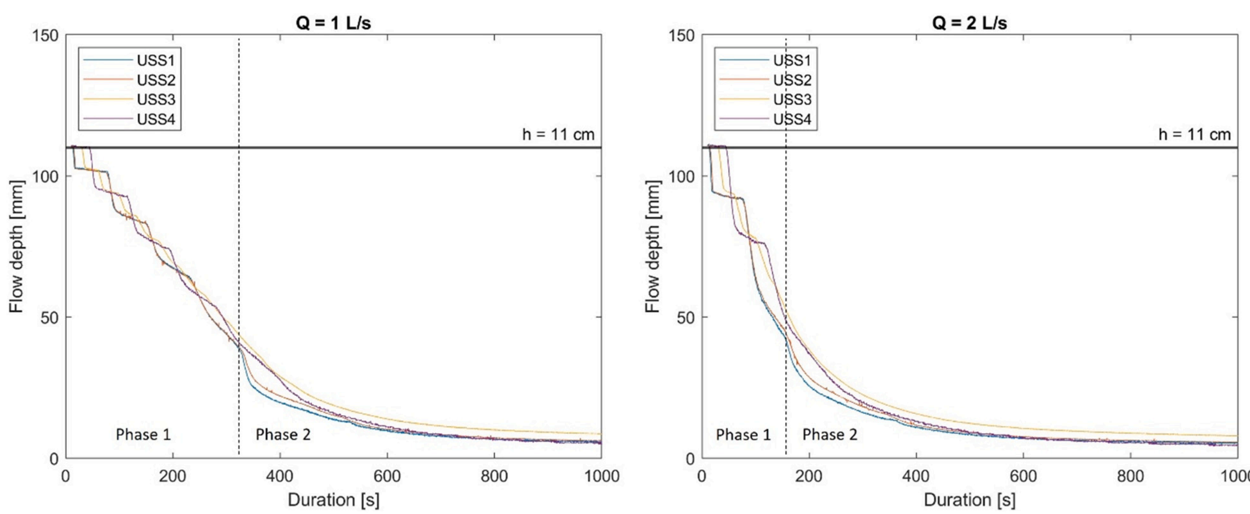

Fig. 13. The flow depth over time during outflow recorded by four ultrasonic sensors (USS1–4). Phase 1: constant mean water-level decrease with oscillating sunk wave; Phase 2: logarithmically decaying water-level decrease approaching zero. Left: Q = 1 L/s, $h_0 = 11$ cm; right: Q = 2 L/s, $h_0 = 11$ cm.

barely be observed.

At an initial water depth $h_0 = 13$ *cm* (Fig. 17), the oscillation height at all USS positions, and flow rates of $Q = 1$ and 2 *L/s* barely differed from the experiments with $h_0 = 11$ *cm* (Fig. 16).

Further increasing the initial water level to $h_0 = 15$ *cm*, thus implementing a larger water body, did not significantly affect the oscillation height. The first oscillation was not recorded because the water level, $h_0 = 15$ *cm* was outside the measurement range of the USSs. At $Q = 1$ *L/s*, oscillations in the inflow and end sections of the flume decreased from approximately 7 *mm* after 100 *s* to 3.5 *mm* after 350 *s* and, in the middle section of the flume, from 2 *mm* to <1 *mm*. At $Q = 2$ *L/s*, two full oscillations were recorded between 40 and 200 *s* after opening the valve at the inflow and end sections of the flume, the first at 16 *mm* and the second at 12 *mm* in height. In the middle section of the flume, the oscillation began at approximately 4 *mm* in height and decreased to approximately 2 *mm* (Fig. 18).

In summary, in the experiments, Phase 1 of the outflow process was not significantly affected by the applied variation in the initial water levels. However, increasing the flow rates led to (i) shorter time periods in Phase 1, and (ii) greater sunk wave oscillation heights, whereas the wave periods remained relatively constant at 70 *s* in the inflow and end sections of the flume, and at 35 *s* in the middle section of the flume throughout the parameter variations.

5.2.2. Phase 2 – approaching the target final water level

If the target final water level was $h_T = 0$ *cm*, Phase 2 of the outflow process was simply a logarithmically decaying water level approaching zero (Fig. 13). In the case of $h_T = 2$ *cm*, Phase 2 also began with a logarithmically decaying water level, but transformed into a surge wave triggered by closing the valve (Fig. 19). The surge wave oscillated through the flume and decayed gradually as it approached the target final water level.

In experiments with $h_T = 4$ *cm*, a logarithmically decaying water level did not occur (Fig. 20). Instead, Phase 2 was initiated by closing the valve, which immediately triggered the development of a surge wave. This wave oscillated again through the flume, decreasing in height until

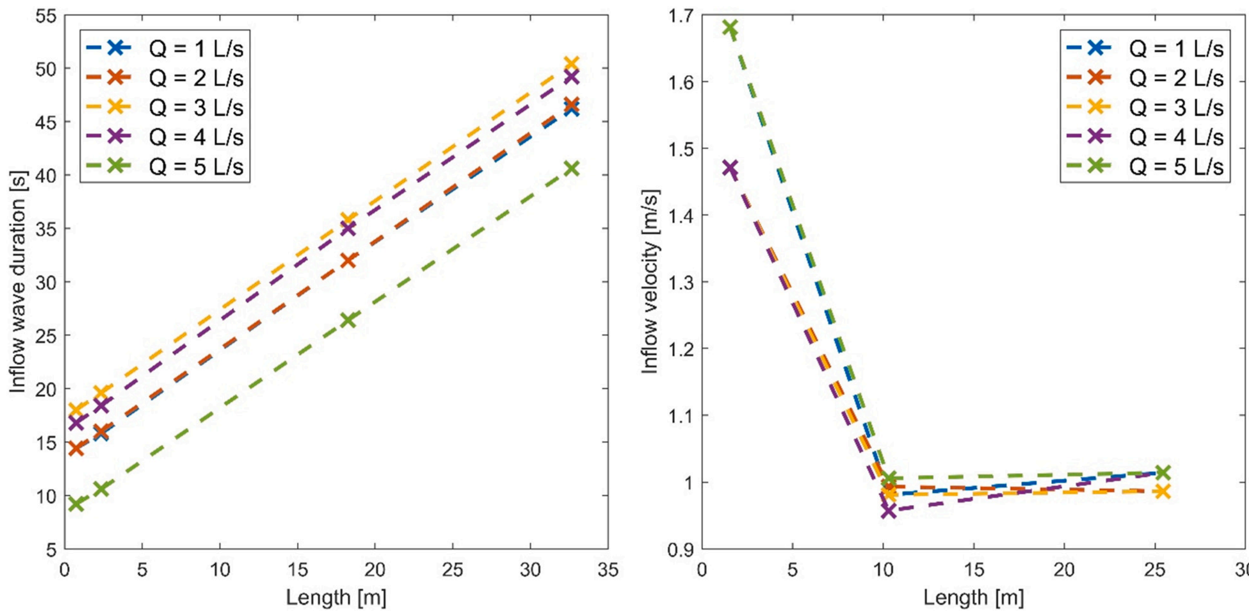

Fig. 14. Outflow wave duration (left) and, outflow velocity (right) over the channel length for experiments with $h_0 = 11$ cm.

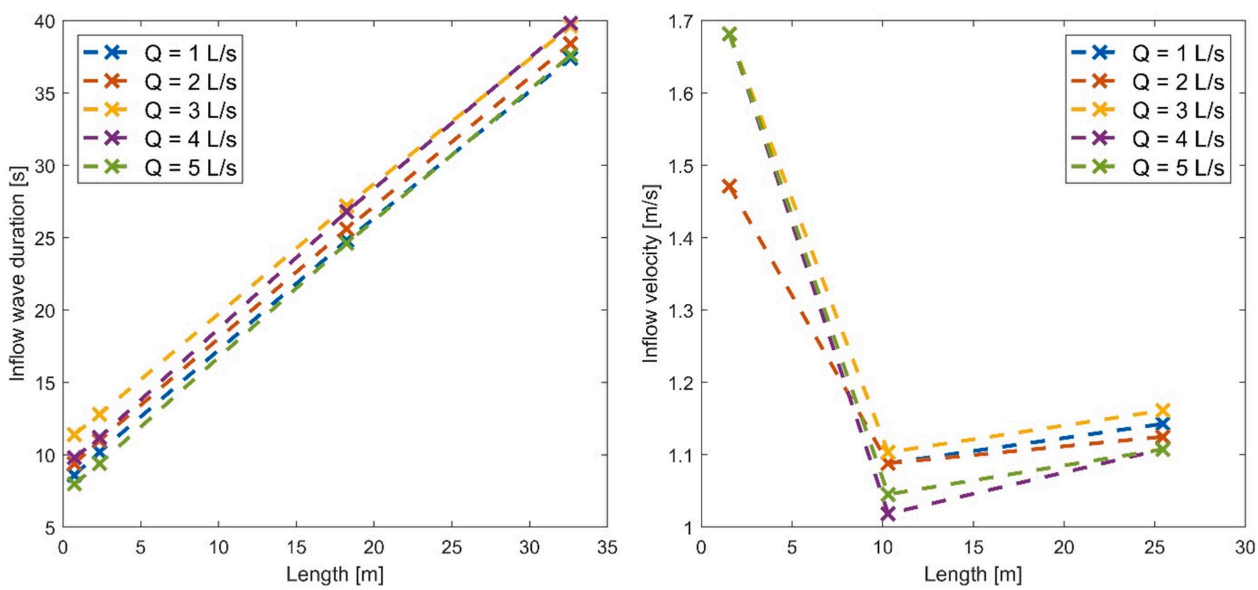

Fig. 15. Outflow wave duration (left) and, outflow velocity (right) over the channel length for experiments with $h_0 = 13$ cm.

the water surface became smooth.

During Phase 2 of the inflow process, the mean wave periods were calculated for the oscillating surge waves during Phase 2 of the outflow process (Fig. 21). Wave periods did not vary significantly with flow rates but depended on the water level. For $h_T = 2$ cm, the wave period was approximately 80–90 s in the middle section of the flume and varied between 160 and 190 s at the inflow and end sections of the flume, whereas for $h_T = 4$ cm, the values of the wave period were approximately 60 s in the middle section of the flume and ranged from 90 to 125 s at the inflow and end sections of the flume.

In Phase 2 of the outflow process, the hydrodynamic processes in the reservoir primarily depended on the water level rather than the flow rate.

6. Discussion

6.1. Basic hydraulic processes in the lower reservoir

In the UPS reservoir model, global and local flow processes occur during the filling and emptying of the lower reservoir, with local processes overlaying global processes [2]. Nevertheless, knowledge of global processes, with a focus on the mean water level, are crucial for operating a UPSH model.

6.1.1. Global processes

The time-dependent mean water level was particularly relevant in Phase 1 of the inflow and outflow processes. Neglecting the oscillations during Phase 1, the water level in the reservoir depends on the initial water level, inflow, time, and geometry of the reservoir and can be calculated using Eqs. (6) (inflow) and (7) (outflow):

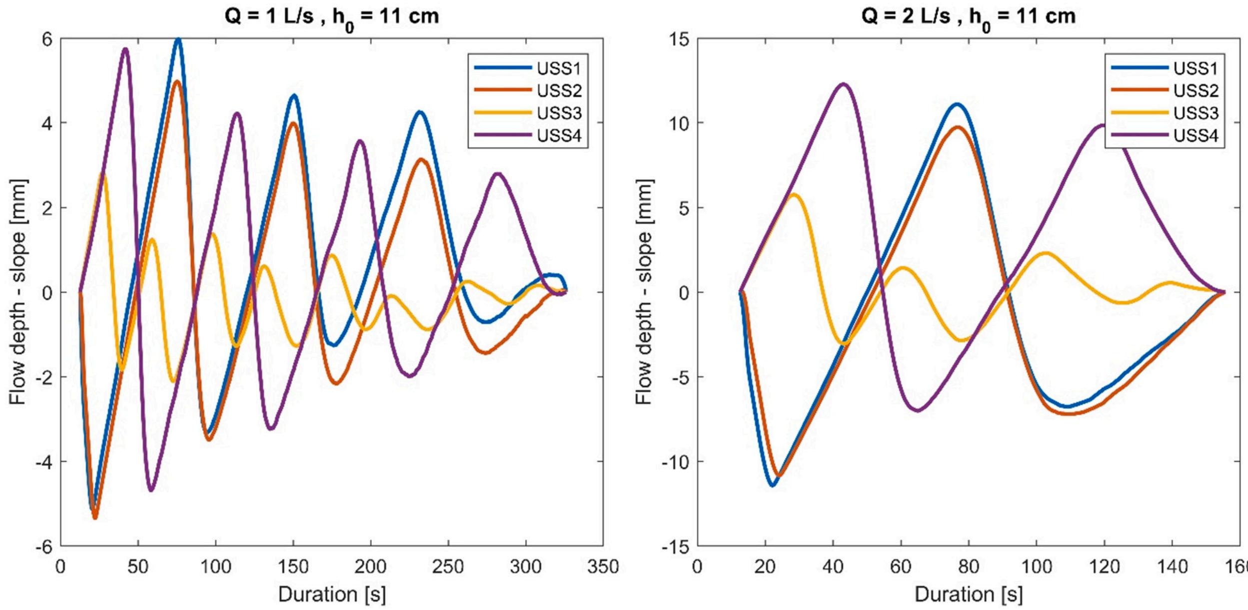

Fig. 16. Oscillations during outflow Phase 1 for h_0 = 11 cm. Left: Q = 1 L/s; right: Q = 2 L/s.

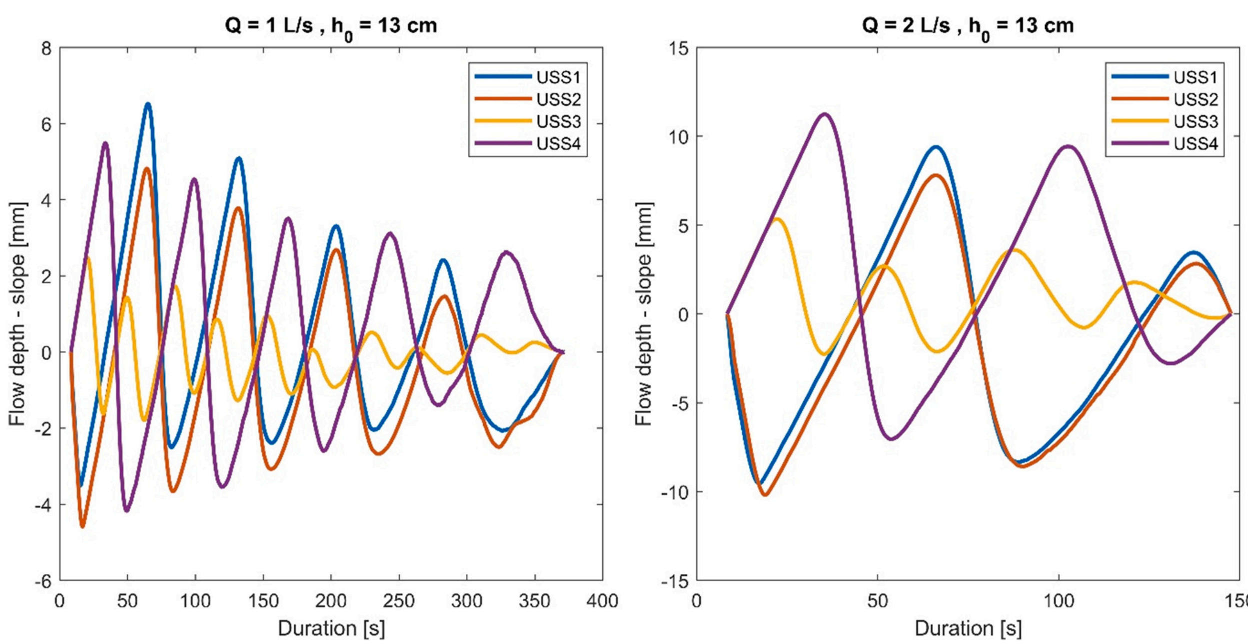

Fig. 17. Oscillations during outflow Phase 1 for h_0 = 13 cm. Left: Q = 1 L/s; right: Q = 2 L/s.

$$h(t) = h_0 + \int_0^T \frac{Q \bullet t}{l_B \bullet w}\, dt \tag{6}$$

$$h(t) = h_0 - \int_0^T \frac{Q \bullet t}{l_B \bullet w}\, dt \tag{7}$$

The measured and calculated water levels are depicted as an example of the filling process of the two experiments in Fig. 22.

The water level during the period of wave damping (Phase 2) can be approximated by Eq. (1), introduced in Section 3.3, which represents a cosine function depending on position x in the longitudinal direction along the flume, and time t in s:

$$h(x,t) = h_T + H\cos\left(\frac{2\pi}{T}t\right)\cos\left(\frac{2\pi}{L}x\right)e^{-\xi\omega_D t} \tag{1}$$

where

$$\begin{aligned} &h_T = target\ final\ water\ level\ [m] \\ &H = wave\ height\ of\ the\ first\ wave\ [m] \\ &T = wave\ period\ [s] \\ &L = length\ of\ the\ flume\ [m] \\ &\xi = \frac{1}{2\pi} \bullet ln(\delta) \\ &\delta = wave\ damping\ factor\ [-] \end{aligned} \tag{2}$$

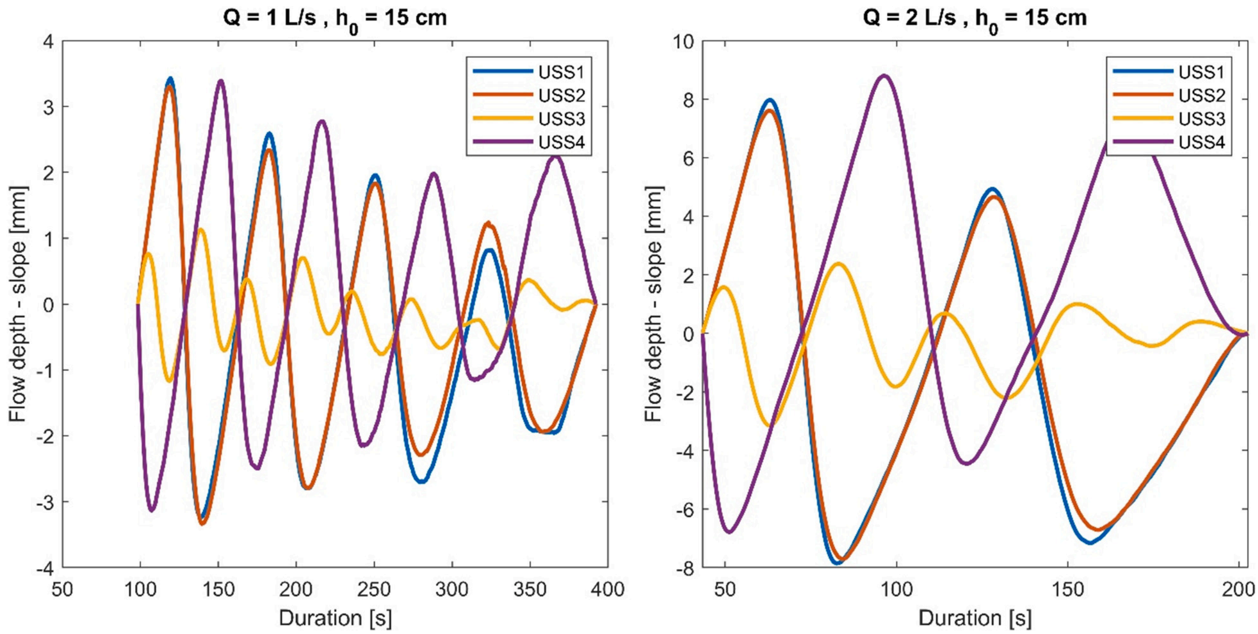

Fig. 18. Oscillations during outflow Phase 1 for $h_0 = 15$ cm. Left: Q = 1 L/s; right: Q = 2 L/s.

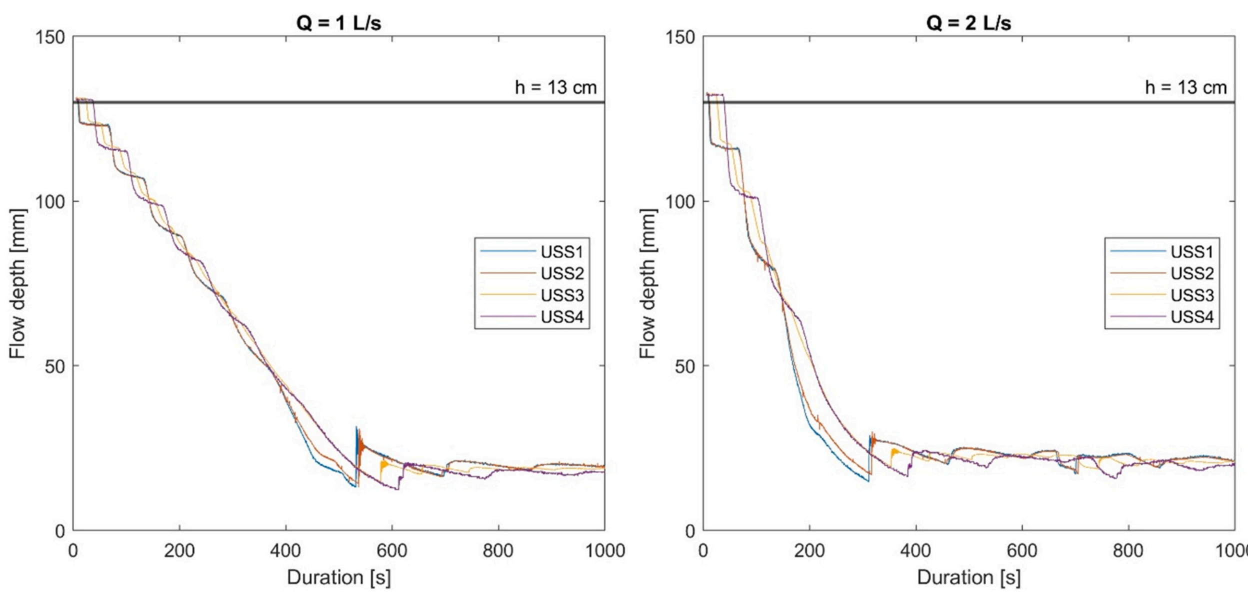

Fig. 19. Flow depth over time during outflow recorded by four ultrasonic sensors (USS1–4). Phase 1: constant mean water-level decrease with oscillating sunk wave; Phase 2: logarithmically decaying water level, followed by an oscillating surge wave. Left: Q = 1 L/s, $h_T = 2$ cm; right: Q = 2 L/s, $h_T = 2$ cm.

$$\omega_D = \omega\sqrt{1-\xi^2} \tag{3}$$

$$\omega = \frac{2\pi}{T} \tag{4}$$

The wave damping factor δ was determined empirically and basically described the height ratio of two consecutive wave crests. For Q = 1 *L/s*, the factor was 1.12 at the positions of USS1, -2 and -4 (inflow and end sections of the flume), and 1.06–1.09 (depending on the initial water level) at USS3 (middle section of the flume). For Q = 2–5 *L/s*, the factor was 1.2 at USS1, -2 and -4 positions, and 1.1 at USS3. The measured and calculated water levels are shown in Fig. 23 and Fig. 24.

To use Eq. (1) for operating a UPSH plant, the wave-damping factor of the reservoir and the height of the first wave should be evaluated.

6.1.2. *Local processes*

Based on the experimental results, three types of waves, which were considered local processes, could be distinguished as basic hydraulic processes: first, surge and sunk waves triggered by opening the valve; second, surge and sunk waves dissipated into single waves owing to reflection at the flume end section, which oscillated through the flume; and third, contained oscillations, which developed after closing the valve, gradually reducing height, and finally approaching a smooth water surface. The wave types are described in detail by Pummer [2] and determined using the Froude number. However, boundary values for different wave types have been described differently in various studies.

6.1.2.1. Local processes – surge and sunk waves. Surge- and sunk-wave development resulted from the valve opening, which caused discontinuities that in turn led to unsteady flows. Regarding the inflow, a

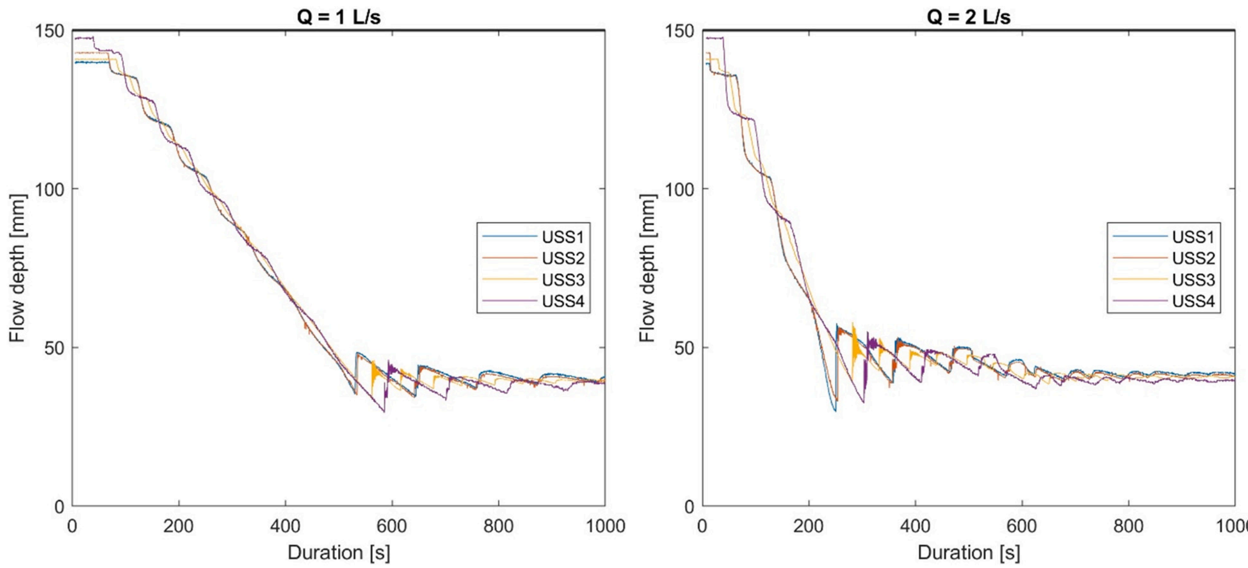

Fig. 20. The flow depth over time during outflow recorded by four ultrasonic sensors (USS1–4). Phase 1: constant mean water-level decrease with oscillating sunk wave; Phase 2: logarithmically decaying water level, followed by an oscillating surge wave. Left: Q = 1 L/s, h_T = 4 cm; right: Q = 2 L/s, h_T = 4 cm.

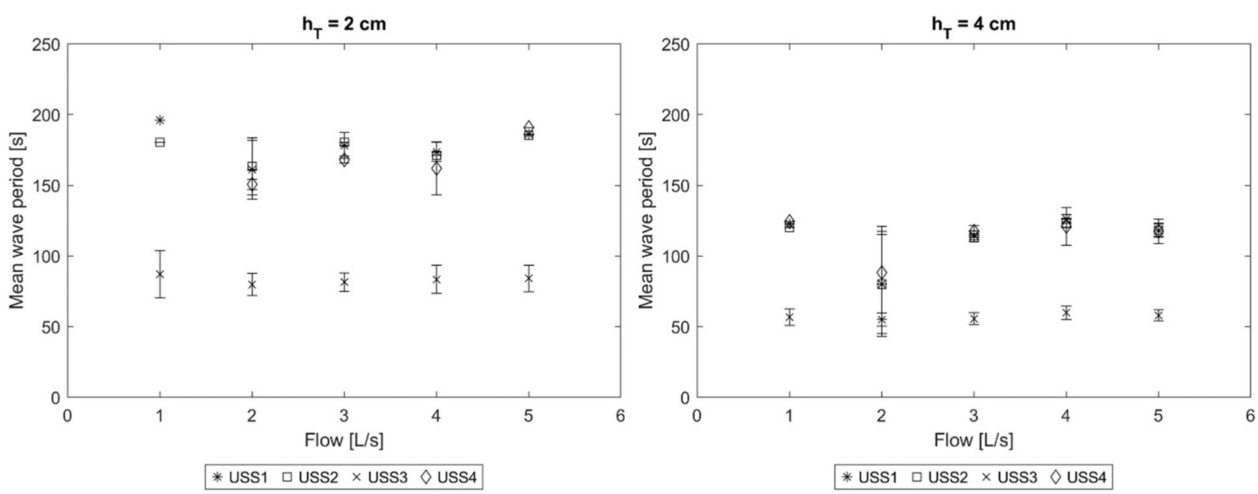

Fig. 21. Mean wave periods with standard deviations during Phase 2 of the outflow of the underground pumped storage reservoir model. Left: h_T = 2 cm; right: h_T = 4 cm.

breaking bore developed owing to the sudden start of the filling process. This can be determined using the Froude number at a position directly downstream from the wave formation:

$$Fr_1 = \frac{\pm v + c}{\sqrt{g \bullet h_0}} \tag{8}$$

where v is the flow velocity = 0 m/s, c is the wave velocity [m/s], and h_0 is the initial water level [m].

For the initial water level $h_0 = 0$ cm, Fr_1 could not be calculated because it was divided by zero. For $h_0 = 2$ cm and $h_0 = 4$ cm, Fr_1 ranged from 1.29 to 2.21 and thus in the order of magnitude of breaking bores with secondary waves, except for the initial parameters $h_0 = 4$ cm and Q = 1 L/s. Fr_1 at the end section of the flume was 1.17, which corresponds to undular bores. Although the surge waves were clearly visible during the experiments, this was not the case for sunk waves. The latter developed flat, inclined wavefronts and reduced their curvatures shortly after formation, leading to large waves [2]. However, the sunk waves were clearly recognizable in the data. Regarding wave velocity, the results showed that the sunk waves proceeded through the flume faster than the surge waves. Throughout the experiments, the inflow and outflow velocities in the pipe were the same for the same Q because the pipe diameter remained constant, and we assumed that the pipe was completely filled. Thus, the "inflow velocity" shown in the results represented the velocity of the surge wave front, whereas the "outflow velocity" referred to the velocity of the sunk wave front. Both wave types exhibited reduced velocities while traveling through the flume. For the sunk waves (Fig. 14 and Fig. 15), a significant velocity reduction occurred in the inflow section of the flume, after which the velocity remained approximately constant. The surge waves reduced their velocity continuously at the initial water level of $h_0 = 0$ cm (Fig. 6), whereas at $h_0 = 4$ cm a strong velocity reduction occurred at the inflow section of the flume (Fig. 8). The velocities of the sunk waves were approximately 1.5 times those of the surge waves. Accordingly, the wavelengths of sunk waves should be greater than those of surge waves, which is in good agreement with the curvature reduction mentioned above.

6.1.2.2. Local processes – oscillating single waves. Owing to the surge- and sunk-wave reflections at the end section of the flume, oscillating

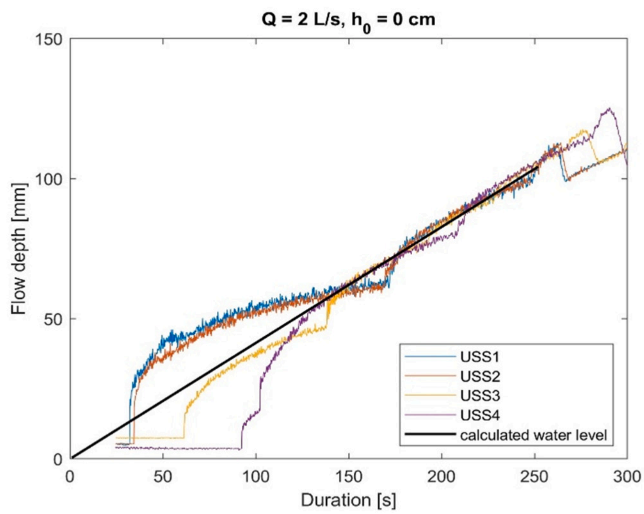

Fig. 22. Measured and calculated (Eq. (6), black line) water levels during Phase 1 in two experiments.

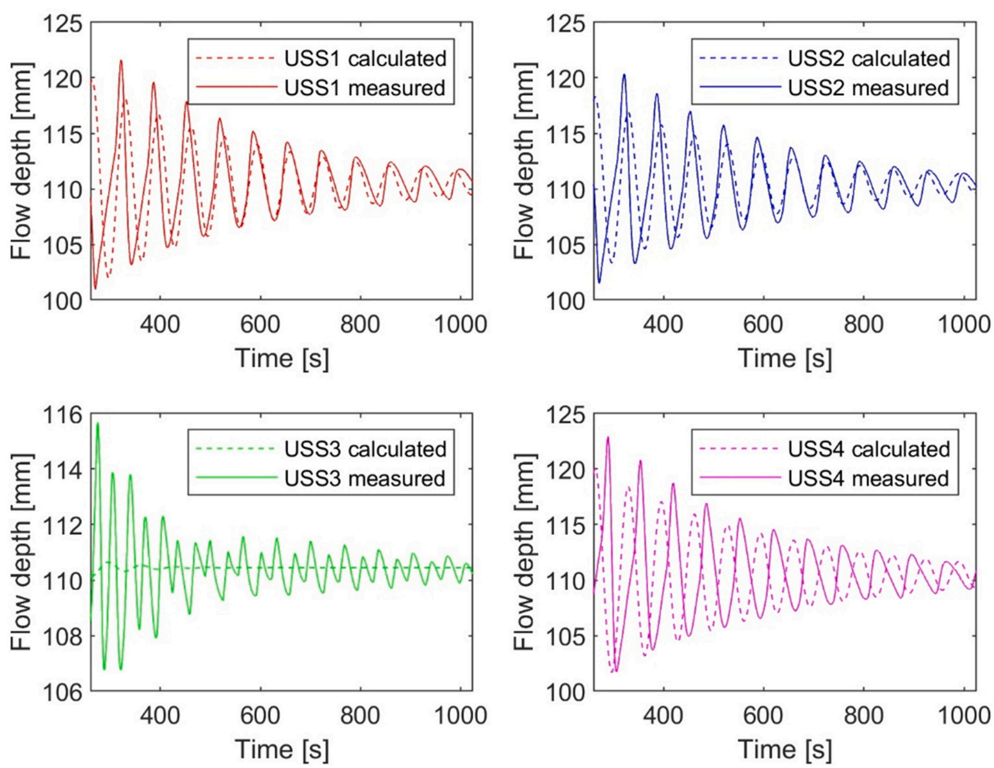

Fig. 23. Measured and calculated (Eq. (1) water levels during Phase 2 of the filling process with Q = 2 L/s and h_0 = 0 cm.

single waves developed during the inflow and outflow, whereas the mean water level increased and decreased relatively constantly. Extracting the oscillations from the mean water-level change revealed wave periods that remained constant at approximately 70 *s* regardless of the initial and actual water levels, flow rate (1, and 2 *L/s*), and process (inflow or outflow). As wave periods typically depend on the flow depth, wave velocity, and wavelength, the obtained results raise questions regarding the parameters affecting the wave periods during these specific inflow and outflow phases in the lower UPSH reservoir. The wave period was related to the channel geometry because this parameter did not change during the experiments.

6.1.2.3. Local processes – contained oscillations. Phase 2 of the inflow and outflow processes was characterized by sunk and surge waves that oscillated through the flume. However, these oscillations differed from those described above, because there was no inflow or outflow. Therefore, the waves oscillated in the closed (but aerated) basin model. This led to the hypothesis that the oscillations were contained, similar to harbor seiches and could be calculated using Eq. (9):

$$T_N = \frac{2 \bullet l_B}{\sqrt{g \bullet h}} \tag{9}$$

where T_N is the wave period [*s*]; l_B is the length of the basin [*m*]; and *h* is the mean water level [*m*].

With regard to the experimental results, the wave periods calculated by applying Eq. (9) and the target final water levels, along with the

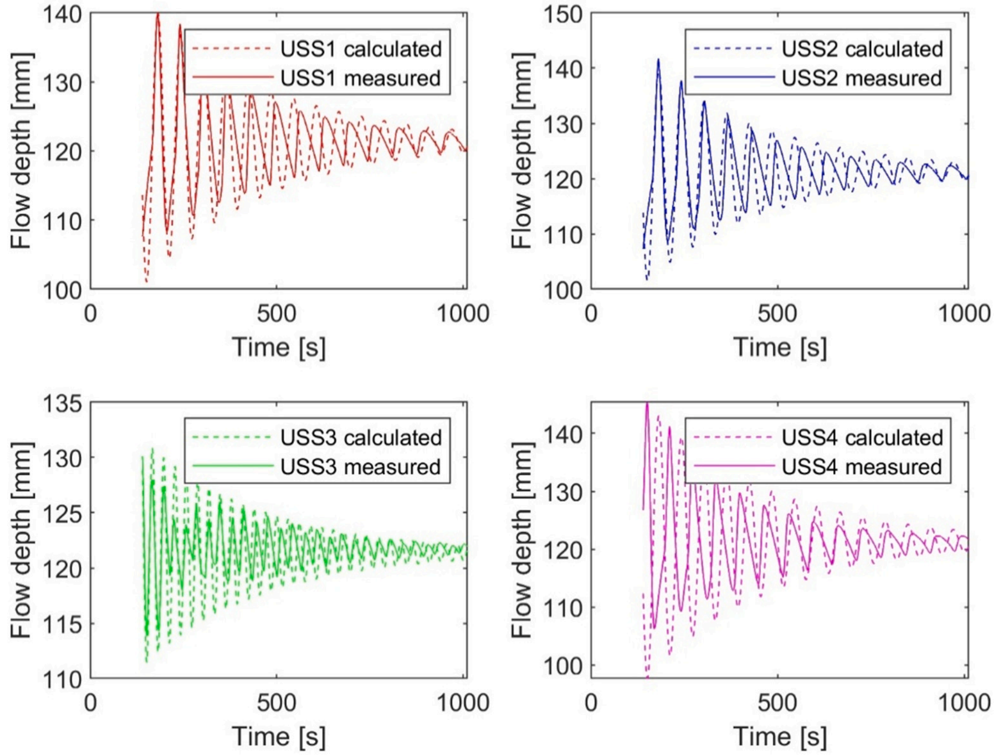

Fig. 24. Measured and calculated (Eq. (1) water levels during Phase 2 of the filling process with Q = 4 L/s and h_0 = 2 cm.

actual final water levels and wave periods for the experiments with $Q = 1\ L/s$ were obtained, as shown in Table 3.

Comparing the calculated and measured values showed that at high water levels (0.11 and 0.13 m) Eq. (9) was well applicable to calculate wave periods. Thus, the waves during Phase 2 of the filling process can be considered to contain oscillations. However, at low water levels, the calculations underestimated the actual wave periods. Hence, the oscillations may be affected by additional parameters such as wall and bottom roughness and surface tensions.

6.2. Model and scale effects

Any experimental investigation should be conducted based on model and scale effects. The model effects result from (i) an approximate representation of the nature, response, and actual structure, and (ii) data acquisition and analysis. Regarding the UPSH model, the differences between the model and actual structure may be, among others, the fluid, which was clean water in the lab and may be sediment-loaded river water in nature, wall roughness, aeration, and channel geometry, as the model was not based on a specific abandoned mine. The flow processes in the model were not affected by the measurement technique, because the USSs measured the water level without water contact.

Scale effects result from different scales in the model and nature, which inevitably lead to a violation of the similarity laws. To transfer the results from the model scale to an actual structure, they can be upscaled using Froude's law (Section 4) under the consideration of scale effects, particularly regarding the effects of viscosity and surface tension.

Table 3
Calculated and measured final water levels and wave periods for Q = 1 L/s.

Target final water level h_T [m]	Calculated wave period T_N [s]	Actual final water level h [m]	Actual wave period T [s]
0.02	156	0.19	188
0.04	109	0.04	121
0.11	66	0.11	67
0.13	61	0.13	62

6.3. Future directions and challenges

This study discusses the hydraulic processes that develop within a basin, similar to the gallery of a disused mine. This study considered basic hydraulic processes, specifically the wave types occurring during the separate inflow and outflow processes of the lower reservoir, supplementing prior research.

Knowledge on basic hydraulic processes occurring in tunnel-shaped lower UPSH reservoirs is essential to ensure safe operation. The hydraulic processes affect the overall energy storage by (i) limiting the maximum possible water level in the reservoir to avoid wave cracking and (ii) by determining the efficiency of the entire system. The results obtained can be used for calibrating a numerical model, which in a next step can be adapted to the geometry of a specific mine to give specific quantitative indications for the UPSH operation.

The increasing use of renewable energy has led to fluctuations in electricity production, and an increasing need for systems that enable rapid switching between storage and electricity production. Therefore, future UPSH plants are likely to be subjected to cyclic processes. Based on the basic hydraulic processes presented in this study, the effects associated with the cyclic processes were investigated in subsequent experiments. These include the effects of many subsequent filling and emptying processes, sudden changes between the filling and emptying of the lower reservoir, effects of ventilation (no ventilation, position, and number of ventilation shafts), overtaking waves, and wave collisions, which should be investigated for safe operation. A study of cyclical processes would have to proceed with an analysis of the statistical significance of the observed effects. In this context, the potential impact of the long-term operation and maintenance of an actual UPSH plant may affect hydraulic processes. These include stability factors associated with changes in humidity and/or stress redistribution and productivity factors such as pressure fluctuations, water surges, and water hammer processes, which could affect all components of a UPSH plant. This was discussed in detail by Colas et al. [8].

All the categories of PSH plants are devoted to increasing clean energy production. The specific category of UPSH plants on which this study focuses is targeted at lower reservoirs where disused mines are available. Implementing an underground pumped storage reservoir in such mines requires detailed knowledge of a variety of disciplines, subjects, and topics, such as the geology and mechanics of the remaining mine formation, as well as economic calculations for project operation and maintenance.

7. Summary and conclusions

The objective of this study was to draw attention to the current necessity to improve our basic knowledge of the essential topics in the hydraulic processes of UPSH that should be resolved before UPSH plants are constructed in abandoned mine areas. To achieve this objective, the authors conducted a short review of the development of the UPSH concept. The decision of the European Union to stop the operation of mines, particularly coal mining, made these areas attractive for application of UPSH plants. This study reviewed the contributions of several groups of researchers suggesting the use of abandoned mines in Germany, Spain, and Belgium for UPSH plants. Special attention was given to the extension of the hydraulic issues represented in the studies reported by these researchers. These issues with additional aspects require further analysis and knowledge improvement. Knowledge of the basic hydraulic processes in the lower reservoir of a UPSH plant is essential to implement safe and efficient operation, but has not been a central topic in recent research. This is the first study to experimentally investigate these processes in a single horizontal cavern-shaped lower reservoir. Basic flow phenomena occurring in the lower reservoir of UPSH plants were investigated using an experimental model shaped like a typical mine cavern but did not represent a specific mine. The primary hydraulic processes occurring during the filling and emptying of the lower reservoir were surge and sunk waves, which dissipated into single waves and finally transformed into contained oscillations. Equations for calculating the water level in the reservoir are introduced, which require verification through additional experiments. This study contributes to filling the gap of knowledge on hydraulic processes in cavern-shaped lower reservoirs of UPSH plants. The physical model allows conducting experiments under controlled initial and boundary conditions. However, the results are limited to the (scaled) geometry of the model. Furthermore, cyclical processes were not considered within this study, but play a crucial role in UPSH plant operation. The model may thus serve for additional investigations.

CRediT authorship contribution statement

Berit Finklenburg: Writing – review & editing, Writing – original draft, Visualization, Validation, Methodology, Investigation, Formal analysis, Conceptualization. **Hillel Rubin:** Writing – review & editing, Writing – original draft, Investigation, Formal analysis, Conceptualization. **Holger Schüttrumpf:** Writing – review & editing, Writing – original draft, Supervision, Resources, Project administration, Funding acquisition, Conceptualization.

Funding

This study was examined within the project "Cyclical Processes in Underground Pumped Storage Power Plants," funded by the German Research Foundation (DFG, grant number 449163970).

Declaration of competing interest

The authors declare that they have no known competing financial interests or personal relationships that could have appeared to influence the work reported in this paper.

Data availability

Data will be made available on request.

References

[1] X. Lyu, T. Zhang, L. Yuan, K. Yang, J. Fang, S. Li, S. Liu, Pumped storage hydropower in abandoned mine shafts: key concerns and research directions, Sustainability 14 (2022) 16012, https://doi.org/10.3390/su142316012.
[2] E.M. Pummer, Hybride Modellierung der hydrodynamischen Prozesse in unterirdischen Pumpspeicherreservoirs, Dissertation, Aachen, 2016.
[3] A. Blakers, M. Stocks, B. Lu, C. Cheng, A review of pumped hydro energy storage, Prog. Energy 3 (2021), https://doi.org/10.1088/2516-1083/abeb5b.
[4] International Hydropower Association, 2025 World Hydropower Outlook: Opportunities to Advance Net Zero, 2025.
[5] International Hydropower Association, Hydropower Status Report: Sector Trends and Insights, 2022.
[6] M. Stocks, R. Stocks, B. Lu, C. Cheng, A. Blakers, Global atlas of closed-loop pumped hydro energy storage, Joule 5 (2021) 270–284, https://doi.org/10.1016/j.joule.2020.11.015.
[7] T. Weber, R. Stocks, A. Blakers, A. Nadolny, C. Cheng, A global atlas of pumped hydro systems that repurpose existing mining sites, Renew. Energy 224 (2024) 120113, https://doi.org/10.1016/j.renene.2024.120113.
[8] E. Colas, E.-M. Klopries, D. Tian, M. Kroll, M. Selzner, C. Bruecker, K. Khaledi, P. A. Kukla, A. Preuße, C. Sabarny, H. Schüttrumpf, F. Amann, Overview of converting abandoned coal mines to underground pumped storage systems: focus on the underground reservoir, J. Energy Storage 73 (2023) 109–153, https://doi.org/10.1016/j.est.2023.109153.
[9] R.A. Fessenden, The commercial solution of the problem of utilising, for the production of power, the energy of solar radiation, the wind and other intermittent natural sources, Electrician 65 (1910) 951–953.
[10] K. Yang, Q. Fu, L. Yuan, Q. Liu, X. He, F. Liu, Research on development demand and potential of pumped storage power plants combined with abandoned mines in China, J. Energy Storage 63 (2023) 106977, https://doi.org/10.1016/j.est.2023.106977.
[11] R.A. Fessenden, 1.247.520, 1917.
[12] S.W. Tam, C.A. Blomquist, G.T. Kartsounes, Underground Pumped Hydro Storage: An Interview, 1978.
[13] H.H. Chiu, L.W. Rodgers, Z.A. Saleem, R.K. Ahluwalia, G.T. Kartsounes, F. W. Ahrens, Mechanical energy storage systems: compressed air and underground pumped hydro, J. Energy 3 (1979) 131–139, https://doi.org/10.2514/3.62426.
[14] R.D. Hammett, E. Hoek, Design of Large Underground Caverns for Hydroelectric Projects With Particular Reference to Structurally Controlled Failure Mechanisms, 1981.
[15] Acres American Incorporated, Preliminary Design Study of Underground Pumped Hydro and Compressed-air Energy Storage in Hard Rock. Volume 1. Executive summary. Final Report, 1981.
[16] R.D. Allen, T.J. Doherty, L.D. Kannberg, Underground Pumped Hydroelectric Storage, 1984.
[17] R. Madlener, J.M. Specht, An exploratory economic analysis of underground pumped-storage hydro power plants in abandoned coal mines, SSRN J. (2013), https://doi.org/10.2139/ssrn.2350106.
[18] R.A. Montero, A. Niemann, D. Schwanenberg, Concepts for Pumped-Storage Hydro-Electricity Using Underground Coal Mines, in: Proceedings of the 35th IAHR World Congress, 2013, pp. 1568–1575.
[19] J. Menendez, J. Loredo, Use of coal mines facilities in Northern Spain for the production of sustainable energy, Int. J. Environ. Sci. 2 (2017) 324–328.
[20] V. Kitsikoudis, P. Archambeau, B. Dewals, E. Pujades, P. Orban, A. Dassargues, M. Pirotton, S. Erpicum, Underground Pumped-Storage Hydropower (UPSH) at the Martelange mine (Belgium): Underground reservoir hydraulics, Energies 13 (2020), https://doi.org/10.3390/en13143512.
[21] E. Pujades, A. Poulain, P. Orban, P. Goderniaux, A. Dassargues, The impact of hydrogeological features on the performance of Underground Pumped-Storage Hydropower (UPSH), Appl. Sci. 11 (2021), https://doi.org/10.3390/app11041760.
[22] O. Dresemann, Challenges for the Construction of an Underground Hydroelectric Power Plant with Electricity Storage (UPSHP) in Terms of Public Acceptance and Technical Aspects - a Summary, FH Münster, 2023.
[23] P.P.N. Uddin, M. Asce, Preliminary design of an underground reservoir for pumped storage, Geotech. Geol. Eng. 21 (2003) 331–355, https://doi.org/10.1023/B:GEGE.0000006058.79137.e2.
[24] X. Lyu, K. Yang, J. Fang, J. Tang, Y. Wang, Feasibility study of construction of pumped storage power station using abandoned mines: a case study of the Shitai mine, Energies 16 (2023) 314, https://doi.org/10.3390/en16010314.
[25] M. Wang, P. Guo, X. Jin, G. Dang, Y. Guo, Y. Li, Evaluation of development potential of pumped hydroelectric storage and geothermal utilization system in abandoned coal mine, J. Cent. South Univ. 31 (2024) 2872–2890, https://doi.org/10.1007/s11771-024-5727-z.
[26] Z. Sun, Y. Zhao, J. Ren, Regional development potential of underground pumped storage power station using abandoned coal mines: a case study of the Yellow River Basin, China, J. Energy Storage 77 (2024) 109992, https://doi.org/10.1016/j.est.2023.109992.

[27] E. Pummer, Water and air waves in very long underground pumped storage reservoirs, in: HYDRO 2017: Shaping the Future of Hydropower, Sevilla, Spain, 2017.

[28] E. Pummer, Hybrid modelling of the hydrodynamic processes in underground pumped storage plants - short version and follow-up developments, Wasserwirtschaft 110 (2020) 22–28.

[29] E. Pummer, H. Schuettrumpf, Reflection phenomena in underground pumped storage reservoirs, Water 10 (2018), https://doi.org/10.3390/w10040504.

[30] S. Terrier, M. Bieri, G. de Cesare, A.J. Schleiss, Surge wave propagation in a common Tailrace Channel for two large pumped-storage plants, J. Hydraul. Eng. 140 (2014) 218–225, https://doi.org/10.1061/(ASCE)HY.1943-7900.0000809.

[31] V.T. Chow, Open-Channel Hydraulics, McGraw-Hill Book Company, New York, 1959.

[32] K. Yang, X. Lyu, C. Xu, J. Fang, M. Duan, Z. Zhang, Research on pumped storage and complementary energy development models for abandoned mines in China, J. Cent. South Univ. 31 (2024) 2860–2871, https://doi.org/10.1007/s11771-024-5716-2.

[33] A. Anderson, Surge shaft stability with pumped-storage schemes, J. Hydraul. Eng. 110 (1984) 687–706, https://doi.org/10.1061/(ASCE)0733-9429(1984)110:6(687).

[34] J. Giesecke, E. Mosonyi, Wasserkraftanlagen, Springer, Berlin Heidelberg, Berlin, Heidelberg, 2009.

[35] J. Menendez, J. Loredo, M. Galdo, J.M. Fernandez-Oro, Energy storage in underground coal mines in NW Spain: assessment of an underground lower water reservoir and preliminary energy balance, Renew. Energy 134 (2019) 1381–1391, https://doi.org/10.1016/j.renene.2018.09.042.

[36] L.R.e. Sousa, L. Gouzhao, P. Cafofo, R.L. Sousa, A.T. Gomes, D. Dias, E. Vargas, Underground pumped hydroelectric schemes: the Madeira Island case, Arab. J. Geosci. 15 (2022) 1–20, https://doi.org/10.1007/s12517-021-09333-z.

[37] R.A. Montero, A. Niemann, T. Wortberg, Underground pumped-storage hydroelectricity using existing coal mining infrastructure, in: Proceedings of the 36th IAHR World Congress, 2015, pp. 3592–3599.

[38] R. Montero, T. Wortberg, J. Binias, A. Niemann, Integrated assessment of underground pumped-storage facilities using existing coal mine infrastructure, in: B. Dewals (Ed.), Sustainable Hydraulics in the Era of Global Change, CRC Press, 2016, pp. 953–960.

[39] J. Menendez, A. Ordonez, R. Alvarez, J. Loredo, Energy from closed mines: Underground energy storage and geothermal applications, Renew. Sust. Energ. Rev. 108 (2019) 498–512, https://doi.org/10.1016/j.rser.2019.04.007.

[40] J. Menéndez, J.M. Fernández-Oro, J. Loredo, Economic feasibility of underground pumped storage hydropower plants providing ancillary services, Appl. Sci. (Switz.) 10 (2020), https://doi.org/10.3390/app10113947.

[41] J. Menendez, J.M. Fernandez-Oro, M. Galdo, J. Loredo, Transient simulation of underground pumped storage hydropower plants operating in pumping mode, Energies 13 (2020), https://doi.org/10.3390/en13071781.

[42] E. Pujades, P. Orban, S. Bodeux, P. Archambeau, S. Erpicum, A. Dassargues, Underground pumped storage hydropower plants using open pit mines: how do groundwater exchanges influence the efficiency? Appl. Energy 190 (2017) 135–146, https://doi.org/10.1016/j.apenergy.2016.12.093.

[43] H. Ye, L. Xiao, Y. Liu, X. Xia, S. Miao, Y. Ding, Abandoned mine pits and underground tunnel-based pumped hydro storage plants: preliminary design and discussion, in: In: 2024 9th Asia Conference on Power and Electrical Engineering (ACPEE), IEEE, Shanghai, China, 2024, pp. 726–730.

[44] L. Huang, Z. Hou, Y. Fang, J. Luo, L. Wu, Q. Wang, Y. Guo, X. Zhang, T. Shi, J. Liu, The development, frontier and prospect of large-scale underground energy storage: a bibliometric review, J. Energy Storage 103 (2024) 114293, https://doi.org/10.1016/j.est.2024.114293.

[45] G. Bollrich, G. Preißler, Technische Hydromechanik, Third., Stark Bearb, Aufl., Verl. für Bauwesen, Berlin, 1992.

[46] D. Aigner, G. Bollrich (Eds.), Handbuch der Hydraulik: Für Wasserbau und Wasserwirtschaft, 2nd ed., Beuth Verlag GmbH, Berlin, Wien, Zürich, 2021.

[47] H. Werkle, Finite Elements in Structural Analysis, Springer International Publishing, Cham, 2021.

[48] C. Paschmann, Hydrodynamische Untersuchungen der Füll- und Entleerungsvorgänge im unterirdischen Tiefspeicher eines Pumpspeicherkraftwerkes anhand eines physikalischen Modellversuchs, Diplomarbeit, Aachen, 2012.

[49] M. Meuleners, Konzeption eines Wasserschlosses zur Optimierung der hydrodynamischen Prozesse in einem unterirdischen Pumpspeicherreservoir, Masterarbeit, Aachen, 2017.

[50] H. Schüttrumpf, H. Oumeraci, Layer thicknesses and velocities of wave overtopping flow at seadikes, Coast. Eng. 52 (2005) 473–495, https://doi.org/10.1016/j.coastaleng.2005.02.002.